



DANISH  
TECHNOLOGICAL  
INSTITUTE

---

# Highly Efficient and Simplified Thermodynamic Cycle with Isolated Heating and Cooling – Cost Optimized (ISECOP)

---

- Final report



**Title:**

Highly Efficient and Simplified Thermodynamic Cycle with Isolated Heating and Cooling – Cost Optimized (ISECOP).

**Prepared for:**

EUDP, project no. 64017-05102.

**Prepared by:**

Danish Technological Institute  
Gregersensvej 2, DK-2630 Taastrup  
Refrigeration and Heat Pump Technology

Technical University of Denmark  
Niels Koppels Allé, Bygning 403, DK-2800 Kongens Lyngby  
Department of Mechanical Engineering

Technical University of Denmark  
Brovej, Bygning 118, DK-2800 Kongens Lyngby  
Department of Civil Engineering

**Project consortium:**

SVEDAN Industri Køleanlæg A-S  
Vengcon ApS  
Alfa Laval Lund AB  
METRO THERM A/S  
Arla Foods amla  
Chr. Møller A/S  
Egå Smede- og Maskinværksted.  
Technical University of Denmark  
Danish Technological Institute (project leader)

November 2020

**Authors:**

Danish Technological Institute:  
Claus Madsen  
Jóhannes Kristófersson  
Christopher Murphy  
Rasmus Borup  
Lars Olsen

Technical University of Denmark:  
Brian Elmegaard  
Wiebke B. Markussen  
René Kofler  
Simon Furbo  
Jianhua Fan  
Ioannis Sifnaios

---

## Table of Contents

1.	Preface.....	5
1.1.	Project details .....	6
1.2.	Short description of objectives and results .....	6
1.3.	Executive summary .....	7
1.4.	Project objectives .....	9
1.5.	Project results, dissemination and utilization of results .....	10
1.6.	Utilization of project results .....	10
1.7.	Project Conclusion and Perspective .....	11
2.	Introduction .....	12
3.	Calculation of system performance .....	13
3.1.	Introduction .....	13
3.1.1.	Background and previous work.....	13
3.1.2.	The system .....	14
3.1.3.	Reader’s guide .....	16
3.2.	Quasi-steady-state modelling .....	17
3.2.1.	The model .....	17
3.2.2.	Gradual heating results .....	17
3.2.2.1.	Test Cases for Screening .....	17
3.2.2.2.	Working fluid and heat pump configuration .....	19
3.2.2.3.	Temperature Glide in Heat Sink .....	20
3.2.2.4.	Temperature lift .....	21
3.2.3.	Gradual heating and cooling.....	22
3.3.	Dynamic modelling .....	24
3.3.1.	Dynamic model .....	24
3.3.1.1.	Heat exchanger .....	25
3.3.1.2.	Compressor .....	26
3.3.1.3.	Receiver .....	27
3.3.1.4.	Valves .....	27
3.3.1.5.	Water tank models .....	27
3.3.1.6.	Pipes .....	28
3.3.1.7.	Pump .....	28
3.3.1.8.	Control strategy of the tank system .....	28
3.3.1.9.	Investigated case study.....	28
3.3.2.	Results.....	28

3.4.	Summary .....	32
4.	Effect of tank design on COP .....	33
4.1.	Introduction .....	33
4.2.	Methodology .....	34
4.3.	COP calculation .....	35
4.4.	Small tanks hot side .....	35
4.5.	Conclusions on small tanks, heating operation.....	45
5.	Small tanks cold side .....	47
5.1.	Conclusions on small tanks, cooling operation .....	50
6.	Large tanks hot side .....	51
6.1.	Conclusions on large tanks, heating operation .....	54
7.	Testing of concept .....	55
7.1.	Test setup .....	55
7.2.	Control principle .....	56
7.3.	Control in the tests .....	57
7.4.	Operation of Tests .....	57
7.5.	Test Results .....	58
8.	Conclusion .....	62
9.	References.....	64
	Appendix 1 - Design Guidelines .....	66
	Appendix 2. Test setup .....	69
	Appendix 3. Thermographic observations of temperature profiles.....	72

## 1. Preface

This report is the final report of the study: "Highly Efficient and Simplified Thermodynamic Cycle with **I**solated Heating and Cooling – **C**ost **O**ptimized (ISECOP)". The objective of the project is to develop a heat pump system with an improvement in the energy efficiency of up to 30 % by using a novel technology where heat pumps are operated together with an optimal usage of storages which will reduce the average temperature level in the heat pump. The payback time for the investment is expected to be 1-3 years depending on the configuration and operating conditions.

This research project is financially supported by the Danish Energy Agency's EUDP programme (Energy Technology Development and Demonstration). Project number: 64017-05102.

The project is carried out in cooperation with Technical University of Denmark and the following industrial cooperating partners: SVEDAN Industri Køleanlæg A-S, Vengcon ApS, Alfa Laval Lund AB, METRO THERM A/S, Arla Foods amba, Chr. Møller A/S og Egå Smede- og Maskinværksted.

The following persons have participated in the project:

- Søren Gram, SVEDAN Industri Køleanlæg A-S
- Peter Anskjær, SVEDAN Industri Køleanlæg A-S
- Erich Weiglhofer, SVEDAN Industri Køleanlæg A-S
- Morten Borg Aadorf, Vengcon ApS
- Henrik Clausen, Vengcon ApS
- Kristian Vulff, Vengcon ApS
- Rolf Christensen, Alfa Laval
- Kasper Korsholm Østergaard, METRO THERM A/S
- Kristian Jensen, Chr. Møller A/S
- Anja Olsen, Egå Smede- og Maskinværksted
- John Olsen, Egå Smede- og Maskinværksted
- Poul Erik Madsen, Arla Foods amba
- Puk Lykke-Møller, Arla Foods amba
- Brian Elmegaard, Technical University of Denmark
- Wiebke Brix Markussen, Technical University of Denmark
- René Kofler, Technical University of Denmark
- Simon Furbo, Technical University of Denmark
- Jianhua Fan, Technical University of Denmark
- Ioannis Sifnaios, Technical University of Denmark
- Claus Madsen, Danish Technological Institute
- Cristopher Murphy, Danish Technological Institute

- Jóhannes Kristófersson, Danish Technological Institute
- Rasmus Borup, Danish Technological Institute
- Lars Olsen, Danish Technological Institute.

The project team would like to thank the EUPD programme (Danish Energy Agency) for supporting the project with valuable inspiration.

### **1.1. Project details**

<b>Project title</b>	Highly Efficient and Simplified Thermodynamic Cycle with Isolated Heating and Cooling – Cost Optimized (ISECOP)
<b>Project identification (program abbrev. and file)</b>	EUDP 2016, Project no.: 64017-05102
<b>Name of the programme which has funded the project</b>	Energiteknologisk Udviklings- og Demonstrationsprogram (EUDP)
<b>Project managing company/institution (name and address)</b>	Danish Technological Institute, Gregersensvej 1, DK-2630 Taastrup
<b>Project partners</b>	SVEDAN Industri Køleanlæg A-S Vengcon ApS Alfa Laval Lund AB METRO THERM A/S Arla Foods amba Chr. Møller A/S Egå Smede- og Maskinværksted. Technical University of Denmark
<b>CVR</b> (central business register)	56976116
<b>Date for submission</b>	30. November 2020

### **1.2. Short description of objectives and results**

*English version*

The objective of the project is to develop a heat pump system with an improvement in the energy efficiency of up to 30 % by using a novel technology where heat pumps are operated together with an optimal usage of storages which will reduce the average temperature level in the heat pump. The payback time for the investment is expected to be 1-3 years depending on the configuration and operating conditions.

Several system designs have been evaluated through a series of simulations with different operating and storage configurations. The most promising system design from the simulations has been built and tested. A test heat pump has been built at Svedan Industri Køleanlæg, and tests have been performed and analysed.

The tests have shown an efficiency improvement of 32 % by the selected test setup. The simulations show that it is possible to obtain an even higher performance improvement with other temperatures and refrigerants.

#### *Danish version*

Formålet med projektet er at udvikle et nyt varmepumpekoncept med en forbedring af energieffektiviteten på op til 30 % ved hjælp af en ny teknologi, hvor varmepumper styres sammen med en optimal brug af varmelagre, som derved reducerer det gennemsnitlige temperaturniveau i varmepumpen. Tilbagebetalingstiden for investeringen forventes at være 1-3 år afhængig af udformning og driftsbetingelser.

Udvalgte systemdesigns er blevet evalueret gennem en række simuleringer med forskellige drifts- og lagerkonfigurationer. Det mest lovende systemdesign fra simuleringerne er blevet bygget og testet. En varmepumpe er blevet opbygget hos Svedan Industri Køleanlæg, og en række tests er blevet udført og analyseret.

Testene har vist en effektivitetsforbedring på 32 % ved den valgte testopsætning. Simuleringerne viser, at det er muligt at opnå en endnu større ydelsesforbedring med andre temperatursæt og kølemidler.

### **1.3. Executive summary**

#### **English**

The project has developed a new combined heating/cooling system that efficiently and continuously produces hot and/or cold water with up to 30 % greater efficiency than conventional systems and generates a possibility of accumulating heat and/or cooling. The ISECOP concept is an extension and improvement of the ISEC concept, developed in a completed EUDP project, due to a similar performance, but with less investments.

Depending on the operating conditions, an efficiency improvement of 10-50 % is shown in the completed EUDP project by employing the tank system for heating. An additional increase of 15 % can be achieved by simultaneous use of the tank system for cooling. A further advantage of the concept is the possibility of accumulating hot and cold water.

In the completed EUDP project, it was shown that the ISEC concept works, and a major performance improvement can be achieved. However, it was also shown that costs of the technology provide some challenges. Based on this framework of the technology, both the temperature operating range and the economy when using this system can be increased significantly.

Thus, the focus of the ISECOP project has been the development of components and the control system to achieve an optimal interaction between the heat pump, the heat storage, and the heat consumption. Indeed, it is possible to construct certain essential components,

e.g. the compressor, in a simpler way (e.g. without capacity control) by using the ISECOP concept.

In relation to the ISEC concept, the new ISECOP concept has been widened in three areas:

First of all, a simpler setup of the tank system has been applied. Instead of two relatively large equivalent containers, one small tank for the charging and a larger storage container have been used. This has a great advantage over the ISEC concept because the efficiency is largely retained, while the tank system, the piping, and the control is simpler and, thus, much less expensive. Additionally, it is expected that in some cases a smaller heat pump can be applied due to the increased performance.

The second area that has been addressed is work on a combined system with both heating and cooling. One possible example of this is cooling of milk in a dairy/farm combined with the production of heat for cleaning purposes. Another example is a process such as flue gas condensation in heating plants where a heat pump can be used for cooling of the flue gas, e.g. from 50 to 30 °C. As an example, the energy can be used for heating of district heating water from 50 to 90 °C. In a traditional heat pump, the condensation and evaporation temperature should then be designed to be about 92 °C and 28 °C, respectively. This large temperature difference will result in a relatively low efficiency factor for traditional heat pumps. In the ISECOP system, the heat pump is connected to a tank system. This tank system allows the heat pump to gradually increase and decrease the condensing and evaporating temperatures, respectively, and thereby minimizing the average temperature differences. This system can increase the efficiency factor with approximately 30 % compared to a conventional heat pump. By using the ISECOP concept, it is also possible to expand the work area as compared with a conventional one-stage heat pump system with respect to the range of temperatures between the hot water out and the cold water in. Indeed, it is possible to achieve greater flexibility by using the ISECOP concept since it is possible to displace the inlet temperature of the evaporator and condenser relative to each other where these temperatures are "locked" in a one-stage plant.

In order to provide a better understanding of how the improvements of the ISECOP concept are obtained compared to the ISEC concept, a brief description of the ISEC concept for heating only with two equivalent sized containers is necessary. In the ISEC concept, when heating one container at a time, the heat pump condenser temperature (and also the evaporation temperature) could be made to vary. Thus, when in the heating operation, a condensation temperature, which is only slightly higher than the liquid average temperature during the heating cycle, is achieved. In conventional continuous liquid heating, this is not possible since the condensation temperature has to be above the temperature of the heated liquid leaving the condenser. This can be realized by the ISEC concept.

The ISEC-concept consists of a system that contains two or more containers. Thus, one container will be heated (charged) gradually while the second container, previously charged, will be drained of heat (discharged). When the second container has been discharged, the first container is fully charged with heat, and the system switches to discharging of the first container, while the second container is being charged. Seen from the heat source and heat sink sides, the conditions are not changed by introducing the

ISEC (or the ISECOP) concept (see illustration below ). This means that seen from the “outside”, the operating conditions are not changed by the introduction of the ISECOP concept.

The main challenges of the ISECOP project are the design and the control of the tank system, i.e. both the new one-tank concept and the simultaneous operation of heating and cooling. The work has also been extended into the heat pump, where the coupling of the heat exchanger to the heat pump has been optimized. Furthermore, the heat pump circuit has been scrutinized with a focus on achieving a relatively simple structure.

The project activities have ranged from theoretical calculations, design and construction of individual components, and overall control strategy, to design of systems for functional analysis and construction of the actual systems in the analysis phase. By bringing together companies with a wide professionalism, it has been ensured that the project has achieved results that no company, institute or university could achieve individually.

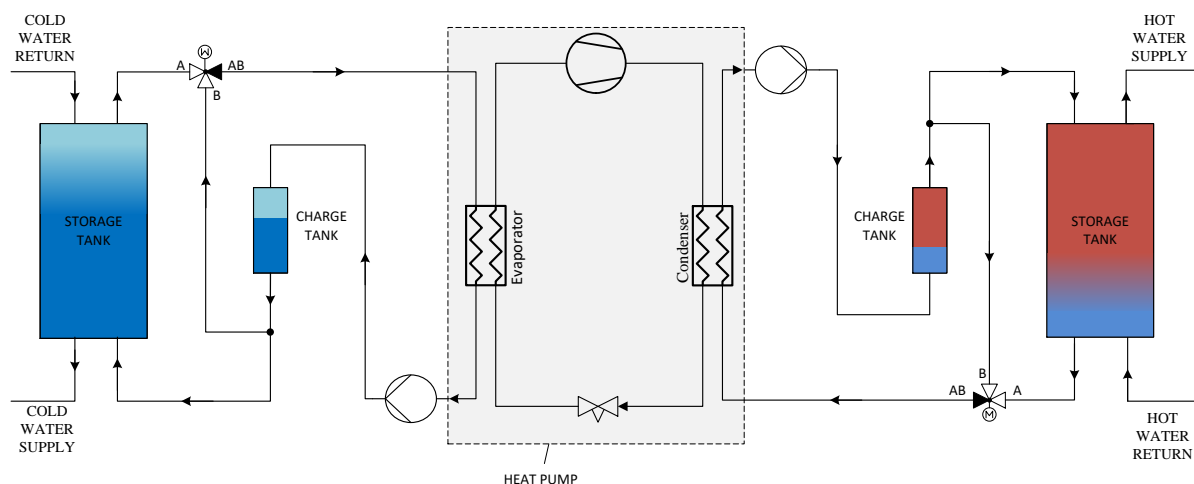


Figure 1: Illustration of the ISECOP concept with simultaneous heating and cooling. The colours show a situation with simultaneous discharging of the charge tanks on both the hot and the cold side.

## 1.4. Project objectives

The aim of the project has been to collect and develop knowledge in the area of using heat pumps in combination with storage tanks for improvement of the performance by gradual heating and cooling. This objective is achieved by carrying out research based on optimization by simulations and testing.

The result is an improved overall performance by the ISECOP concept compared to traditional system designs.

The project experienced different difficulties. The original planned host for the test setup did not have the possibility to be the host due to a business related change. The next plan for a host showed to be impossible due to technical and practical reasons. The third host experienced problems due to a delay caused by the Corona virus. But even due to these problems and delays, it was possible to obtain the expected results from the testing.

## **1.5. Project results, dissemination and utilization of results**

In the project, the ISECOP concept is elaborated by carrying out research encompassing both calculation of the performance and experimental work with different configurations. Also, a calculation tool has been developed.

The objectives stated in the project proposal have been obtained by the conducted research, which shows that the technology is feasible for the intended purposes.

A large number of simulations have been carried out on various potential system configurations. A test setup has been built whose purpose was to document the benefits of the concept. A control system has been built with an associated data acquisition system, so it was possible to operate the heat pump for the purpose and to be able to document the expected COP.

The expected efficiency improvement was 10 to 30 % compared to a traditional heat pump system. Simulations have shown a maximum improvement of as much as 35 %, depending on the selected temperature set, configuration, and refrigerant. The work has shown that it is possible to achieve an efficiency improvement of 32 % by using the ISECOP concept at typical temperature conditions.

In the application, two system configurations are described, one combined heating and cooling and one one-sided with heating. Both were simulated in the project. The one-sided with heating turned out to be the preferred configuration, and this is why only this one was built and tested.

The test setup was not built for the purpose that the system could be used directly as a final design. The system should only be able to document that the concept worked, which it has been able to do, but a commercial product optimized for individual tasks still remains.

## **1.6. Utilization of project results**

The results obtained in the project have documented the potential stated in the application. However, as indicated in section 1.5, there are still several issues which remain to be solved and developed before a final design of the ISECOP concept is completed.

The benefits of using the ISECOP concept are both increasing the efficiency of heat pumps, the application of the concept on both the warm and the cold side, a possible increased temperature lift, a larger capacity of the heat pump due to the increased efficiency, and an increased possibility for flexible energy consumption due to the capability for storing of the heated water.

The final result of all the benefits is that the concept will have a favorable economy compared to traditional heat pump systems. Due to the gained benefits observed in the project, the project participants, involved companies and other stakeholders will be able to adapt the ISECOP concept in their planned heat pump projects.

## 1.7. Project Conclusion and Perspective

The primary purpose of the project has been to provide a basis for the ISECOP concept by using a combination of a heat pump with a storage in an optimal way. This objective has been fulfilled by doing research as a basis for developing a design guide, a calculation tool and a control system followed by an experimental verification of the performance and the benefits of the concept.

The advantage of the ISECOP concept of using gradual heating instead of having heating in only one step has been demonstrated in the project. The theoretical studies have been made which support the solution of designs of the system, e.g. regarding the physical setup of the tank system. The optimal design of the system has been devised which allows to achieve a relative stable outlet temperature. The calculation tool will make it possible to predict the expected efficiency improvement of the system.

Measurements have been carried out on the test set-up, which has demonstrated the feasibility of ISECOP concept, and the results have fulfilled the expected potential.

The prospects are great because it is possible to use the concept for many applications. Both for heating or cooling alone and in combined heating and cooling systems. This means that the concept is applicable from small scale installations for e.g. heating of buildings to larger industrial applications as well as for district heating and cooling installations.

It is expected that the system will be competitive now, but an increased experience from continuous long-term operation will further increase the feasibility and the competitiveness of the ISECOP concept.

The concept will be advantageous for the national strategy for an increased application of electricity with a large efficiency for heating purposes. Due to the increased efficiency and competitiveness, the ISECOP concept is expected to be applied further in the future.

## 2. Introduction

In this project, the aim has been to develop a new heat pump concept using gradual heating by application of storage tanks. The gradual heating will provide a significant boost in system efficiency compared to a traditional system where the temperature lift is done in steps, due to an, in average, smaller difference between the evaporation and condensing temperature.

The system is operated by letting the water in the storage tank pass the evaporator or/and the condenser in a number of cycles. Thereby, the water will gradually be heated and/or cooled. The number of cycles will influence the performance of the system. A small number of cycles will limit the possible efficiency improvement, while a large number of cycles might increase the power used for circulating the water flow and increase the mixing in the storage tank.

The design of a system will also include considerations on how long time the tank volume will have to pass the evaporator/condenser. A small time will lead to a large flow and the reverse with a large time. The circulation time and the number of circulations will decide the necessary tank size.

An ideal performance of the storage tank would be to have a sharp limit between hot water above the limit and cold water below the limit. In practice, this sharp limit is disturbed by vertical mixing in the water, by vertical conduction in the water and wall material in the storage tank as well as influence of the heat capacity of the tank wall material and heat loss to the ambient. The influence of these parameters has been analysed by calculations.

Another issue of large importance is the operation of the system. Due to the request for not stressing the heat pump too much it is necessary to shift the temperature in the evaporator/condenser relatively slowly. The request is generally to have one minute for this change of temperature in the condenser from the highest to the lowest level. This can be done by, after the charge period, having a small water flow at the start of the discharge period to reduce the flow through the condenser in order to have a slow decrease of the temperature out of the condenser. In this phase of the operation, the COP is expected to be relatively low. Therefore, the time used for this shift in temperature should be relatively short in relation to the total time used for charging of the storage tank.

Another operation consideration is the necessary uniformity of the temperature in the charge tank. The COP is lower at the end of the charge period which will lead to a lower temperature difference across the condenser which will also lower the temperature difference between the top and the bottom of the charge tank. This temperature difference can be lowered further by increasing the flow through the condenser when the charge period is close to the end. If the end result is a temperature difference in the charge tank that is still too large it will be possible to further reduce this by adding a bypass between the top of the charge tank and the bottom. After a circulation time corresponding to about one half of the charge tank volume, the temperature in the tank will be relatively uniform.

### 3. Calculation of system performance

#### 3.1. Introduction

##### 3.1.1. Background and previous work

Many countries aim to reduce the use of fossil fuels. The long-term Danish energy policy aims for a fossil fuel free society by 2050. This includes all sectors, also the heating and transport sector. Bühler et al. [1] conducted an energy and exergy analysis of the Danish industry sector. The results show potentials for reduction of fossil fuel use and exergy losses through waste heat recovery and the use of alternative technologies.

Heat pumps (HPs) allow for an efficient, fossil fuel free production of heat, when using electricity from renewable energy carriers like wind and solar. Additionally, HPs allow for process integration by using waste heat streams, which have to be cooled down, while heating another stream at a higher temperature level. The cooled stream could be a warm stream, which is cooled down to ambient conditions before releasing it to the environment. It could also be a stream used for cooling purposes within the same process.

Units providing heating and cooling capacity are referred to as co-generation HPs. The efficiency of such units is typically limited due to the high temperature lift between the cold and hot process water. In order to improve the efficiency of these systems, different cycle configurations, working fluids or new system designs can be used. One interesting approach is serial or gradual heating of water. Gradual heating leads to lower condensing temperatures on average and hence to higher coefficient of performance (COP) compared to heating in one step with conventional heat pumps.

Wang et al. [2] conducted a comparison between a one-stage cycle, a two-stage cycle with intercooler and serial heating by two serial, one-stage HPs. The results show that below a specific temperature lift, the two-stage cycle achieves the highest COP, while a configuration with two HPs in series is the most efficient above the threshold. Ommen et al. [3] investigated the technical and economic feasibility of serially connected industrial HPs. It is shown that serial connection of two or three HPs leads to higher COPs and lower net present values (NPV) compared to one single HP.

Serial heating can also be realized by using storage tanks instead of several HPs in series. This approach is presented by Rothuizen et al. [4] and Olsen et al. [5] termed the ISEC concept and by Löffler and Griessbaum [6] termed the trapezoid cycle. In both concepts, two storage tanks are used, where one tank is charged gradually, until it is fully charged with water of the wanted supply temperature. In the meanwhile, the second tank is discharged, delivering hot water to the process from the top of the tank, while colder return water is filled into the bottom of the discharge tank.

The ISEC concept shows an improvement potential of up to 25 % in COP compared to a conventional HP, where a one-stage HP working with ammonia (R717) was used to heat water from 40 °C to 80 °C with an evaporation temperature of 22 °C [4]. The ISEC concept was furthermore tested experimentally, investigating the performance of the HP and the stratification in the storage tanks [7], [8].

Experimental investigations of the trapezoid cycle show COP improvements of 10 % - 50 % for water inlet temperatures at the condenser between 12 °C – 37 °C. The supply temperature of the hot water and the inlet temperature to the evaporator were kept constant at 42 °C and 10 °C, respectively. A one-stage HP using R134a was used for the experiments [6].

In this project, a system similar to the described systems using storage tanks was investigated. The main difference of the new system to the ones proposed by Rothuizen [4] and Löffler [6] was a different setup of the storage tanks. Additionally, the use of storage tanks on the cold side for simultaneous gradual heating and cooling was investigated.

### 3.1.2. The system

In Figure 2, the heat pump system using a storage system for gradual heating is shown, and the two different operation modes of the tank system at the hot side are depicted. The red solid lines show the water flow during the charging process of the charge tank. In this period, colder water is taken from the bottom of the charge tank, heated in the condenser of the HP, and the hot water is returned to the top of the charge tank. In the meanwhile, hot process water at the required supply temperature is delivered to the process from the top of the stratified storage tank. The cold water returning from the process is fed to the storage tank at the bottom in order to ensure stratification within the tank.

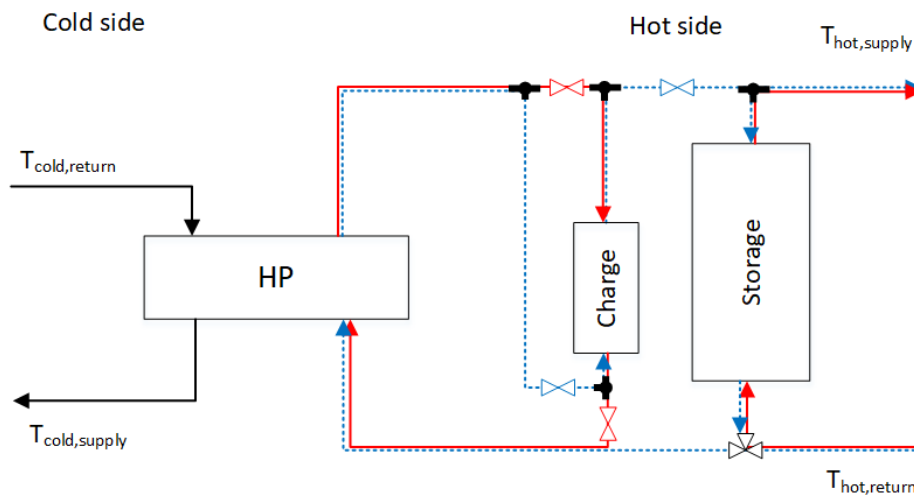


Figure 2: Principle sketch of the system. The red solid line at the hot side denotes the flow during the charging process of the charge tank and the blue dashed line the one during discharging.

When the charge tank is filled completely with water at the required supply temperature, the operation mode is switched to discharge the charge tank. This is shown in Figure 2 with blue dashed lines. In this mode, the return water from the process flows together with water from the bottom of the storage tank to the condenser of the HP. The heated water is then fed to the bottom of the charge tank. The stratification within the charge tank leads the hot water to exit the charge tank at the top. One part of the hot water flow is supplied to the process, and one part of the flow goes into the storage tank in order to refill it. When

all the water at supply temperature has left the charge tank, the charging process of the charge tank starts again.

In Figure 3, the inlet and outlet temperatures to and from the condenser of the heat pump are depicted. In this case, the water is heated in three steps from the return temperature to the supply temperature of the process. With arrows, the definition of one circulation and one charging cycle is shown.

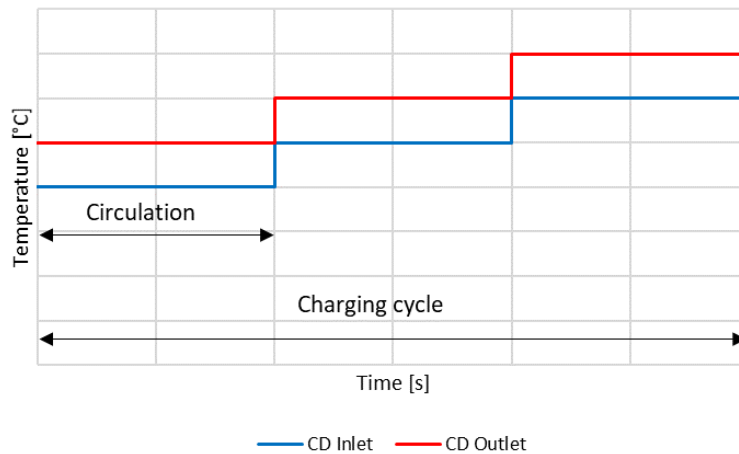


Figure 3: Condenser inlet and outlet temperature during one charging cycle with three circulations.

By connecting a tank system to the condenser and another, working with the same principle, to the evaporator, gradual heating and cooling can be achieved simultaneously. Figure 4 depicts the setup of such a system.

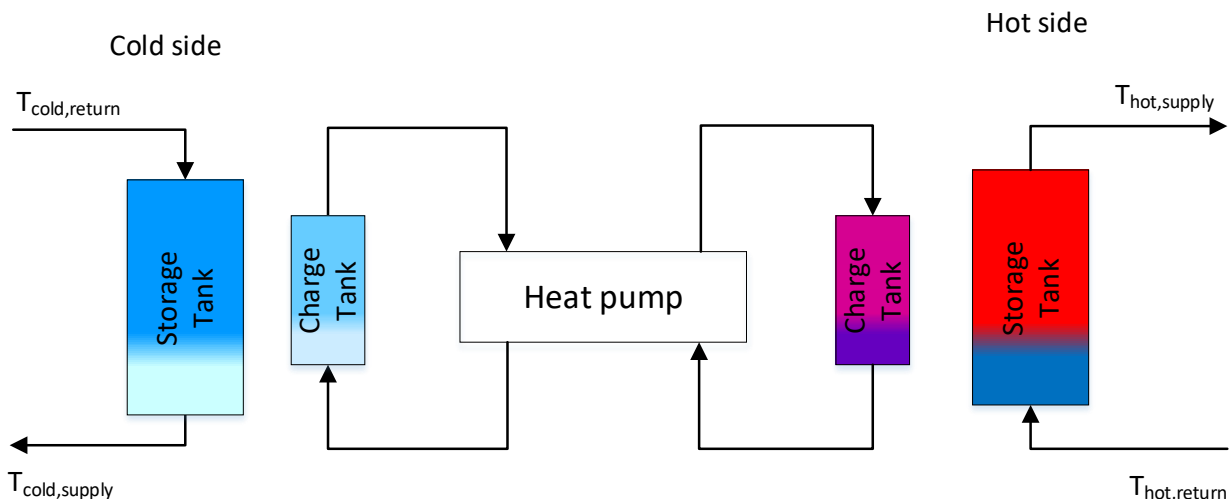


Figure 4: Principle sketch of system for gradual heating and cooling.

Figure 5 shows how the evaporation and condensation temperature of a co-generation heat pump behave over time. For a conventional heat pump, the evaporation and condensation temperatures stay constant throughout the operation. For a system with a tank system connected only to the condenser (gradual heating), the condensation temperature increases step by step, while the evaporation temperature stays constant. When

connecting the tank system on the hot and the cold side (gradual heating & cooling), the condensation temperature increases stepwise, while the evaporation temperature decreases.

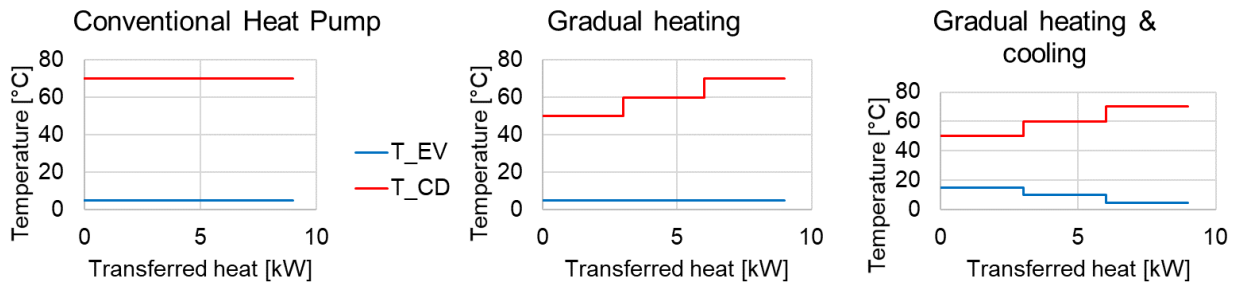


Figure 5: Differences in evaporation and condensation temperature over time between a conventional heat pump, gradual heating only, and gradual heating and cooling.

Figure 6 depicts the theoretical performance of the three systems, expressed with the Carnot COP, calculated as:

$$COP_{Carnot} = T_{CD} / (T_{EV} - T_{CD}) .$$

It shows that by decreasing the temperature lift, the COP of each step increases, leading to the highest COPs for the case with gradual heating and cooling, followed by gradual heating, and eventually the conventional heat pump, reaching the lowest COP.

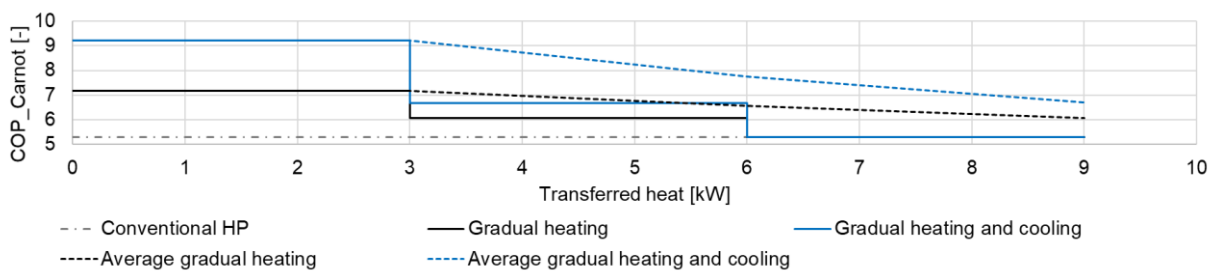


Figure 6: Theoretical comparison of coefficient of performance of a conventional heat pump, gradual heating only, and gradual heating and cooling.

### 3.1.3. Reader's guide

After having presented the background and the basic concept of the project, the main outcomes are presented. The outcomes are divided into two parts. In section 3.2, the quasi-steady-state modelling is presented. This includes a short description of the models built for the system for gradual heating and gradual heating and cooling (section 3.2.1). Thereafter, the results for the performance evaluation of gradual heating (section 3.2.2) and gradual heating and cooling (section 3.2.3) are presented. In section 3.3, the dynamic modelling is presented, including a model description in section 3.3.1 and the results in section 3.3.2.

## 3.2. Quasi-steady-state modelling

In order to assess the potential of the ISECOP system, quasi-steady-state models of the system were built. These models can be used to calculate the maximum achievable COPs through gradual heating or gradual heating and cooling in a real system and compare them to the COP of conventional heat pumps. The models built and used are explained in section 3.2.1. Section 3.2.2 and 3.2.3 show results obtained with the models.

### 3.2.1. The model

Within this project, a model for evaluating the maximum achievable COP with the ISECOP system was built. The model was implemented in the software Engineering Equation Solver (EES) [9]. A detailed description of the models and their abilities, including a detailed user's guide, was elaborated and can be found in Appendix A [10].

The model enables the user to evaluate the performance of a heat pump system by varying the following parameters directly from a graphical user interface:

- Heat pump configuration
- Working fluid
- Tank setup
- Compressor model
  - o Real compressor characteristics
  - o Manually adding polynomials
  - o Generic piston compressor characteristics
  - o Constant efficiencies
- Heat exchangers
  - o Fixed overall heat transfer coefficient UA
  - o Fixed design pinch point temperature difference.

The model was built for robust and quick simulations and enables the user to investigate the COP improvement potential of gradual heating and gradual heating and cooling for any case.

### 3.2.2. Gradual heating results

In this section, results for the screening of the influence of different parameters on the performance of heat pump systems with gradual heating using the model introduced in the previous section are shown. The study was presented the 25th IIR International Congress of Refrigeration 2019 and published by Kofler et al. [11].

#### 3.2.2.1. Test Cases for Screening

In this work, different screenings were conducted. The first screening investigated the performance of the system for different working fluids and cycle configurations for different numbers of circulations per charging cycle of the charging tank. For this screening, cold water was cooled from 20 °C to 10 °C while heating water from 20 °C to 60 °C at the hot side. The number of circulations was varied from 2-15 and then compared to the direct heating HP without a tank system. The examined working fluids were R134a, R290, R600a, and R717. For all working fluids, calculations with a simple one-stage HP were conducted.

For R717, a two-stage cycle with open intercooler and, for the other working fluids, a one-stage cycle with internal heat exchanger (RHE) were investigated additionally.

In the next screening, the influence of the temperature glide in the heat sink was examined. The temperature glide in the heat sink is defined as the difference between the return and supply temperature on the hot side. For the variation, the supply temperature was held constant at 60 °C, while the return temperature was varied from 20 °C to 55 °C. The temperature of the heat source was kept constant.

Finally, the influence of the temperature lift was examined by varying the hot supply temperature between 40 °C and 80 °C while keeping the temperature glide in the heat sink at 20 K. The temperature lift of the process is defined as the difference between the supply temperature and the return temperature of the cold water. By keeping the cold side at the supply temperature of 10 °C and a return a temperature of 20 °C, temperature lifts of 20 K to 60 K were investigated.

For the cases using ammonia (R717) as a working fluid, a flooded evaporator was modelled, assuming a vapor quality of  $x=1$  at the inlet of the (low-stage) compressor. For other working fluids, a direct expansion evaporator with a compressor suction superheat of 5 K was modelled. The operating limits for the compressors were defined with maximum compressor discharge temperatures of 180 °C [3].

In the design run of the evaporator and the condenser, pinch point temperature differences of 5 K were used. The internal heat exchanger effectiveness was fixed to 0.6. For the calculation of the power consumption of the hot water pump, a pressure drop in the condenser of 0.5 bar and an isentropic efficiency for the pump of 0.8 were assumed.

For the cycles working with R717, compressor data from Sabroe were used. For the other working fluids, a compressor from GEA Bock were used. The names of the compressors are shown in Table 1 together with the previous explained assumptions. The data for the fitting of the compressor polynomials were taken from [12] and IPU [13] for the Sabroe and Bock compressors, respectively.

Table 1: Fixed input variables for heat pumps and water pump

Working fluid	R717	R134a, R290, R600a
Compressor suction superheat [K]	0	5
Max. discharge temperature [°C]	180	180
Pinch point temperature difference [K]	5	5
Internal heat exchanger effectiveness [-]	-	0.6
Water pressure drop in condenser [bar]	0.5	0.5
Pump isentropic efficiency [-]	0.8	0.8
Compressor model (one- and high-stage)	Sabroe HPX-708	Bock EX-HG 12P/60 4S
Compressor model (low-stage)	Sabroe SMC-112L	-

### 3.2.2.2. Working fluid and heat pump configuration

In the first screening, the influence of the working fluid and the HP configuration on the COP of the system was examined. Figure 7, right, shows the COP of the conventional HP as colored columns for different working fluids and HP configurations. As seen, changing the HP configuration from one-stage to two-stage or including a RHE leads to an improvement in COP for each working fluid. The boxes on top of the columns show the range of COPs when using the tank system for gradual heating with a different number of circulations of water through the charge tank until it is completely charged.

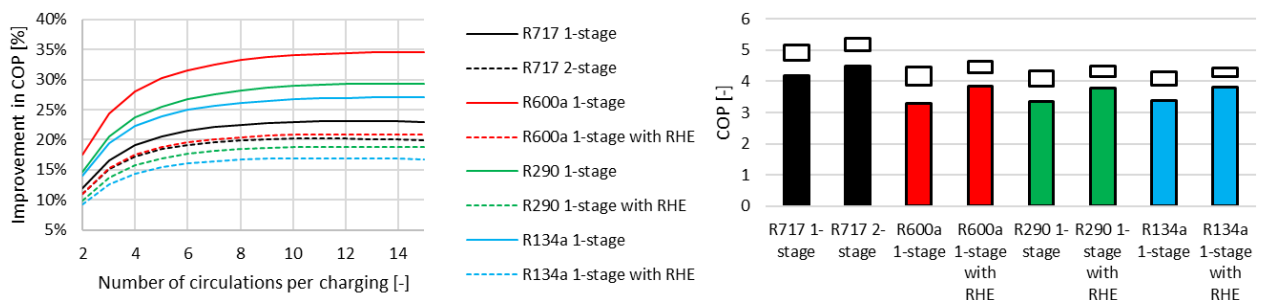


Figure 7: Left: Improvement in COP compared to conventional heat pump for different working fluids and heat pump cycles. Right: Coloured column depicts the COP of a conventional heat pump, the box on top the range for different numbers of circulations during charging.

Figure 7, left, shows the improvement of COP compared to a conventional HP for different working fluids and HP configurations and different numbers of circulations per charging cycle of the charge tank. The solid lines denote the improvement when using a simple one-stage HP and the dashed lines for two-stage HPs or with a RHE. It may be seen that the use of the tank system leads to bigger improvements for the simple one-stage HP configuration than for the other configurations. The difference in improvement between one-stage and two-stage HPs is smaller than between the one-stage HPs with and without RHE. It is also visible that different working fluids show different behavior. The biggest improvement in COP was achieved for a one-stage HP with R600a with an improvement of up to 35 % and a minimum improvement for two circulations per charging cycle of 18 %.

### 3.2.2.3. Temperature Glide in Heat Sink

As a second parameter, the temperature glide in the heat sink was examined. Figure 8, left, depicts the maximum improvement in COP compared to a conventional HP for different temperature glides in the heat sink, working fluids and HP configurations. The values for a temperature glide of 40 K correspond to the maxima of the curves in Figure 7, left. It may be seen that the maximum improvement decreases with decreasing temperature. At a temperature glide of 5 K, the improvement for a one-stage HP with R600a is only 1.2%. For a two-stage heat pump with R717 or an internal heat exchanger with R290 and R134a, no improvement is achieved for a temperature glide of 5 K.

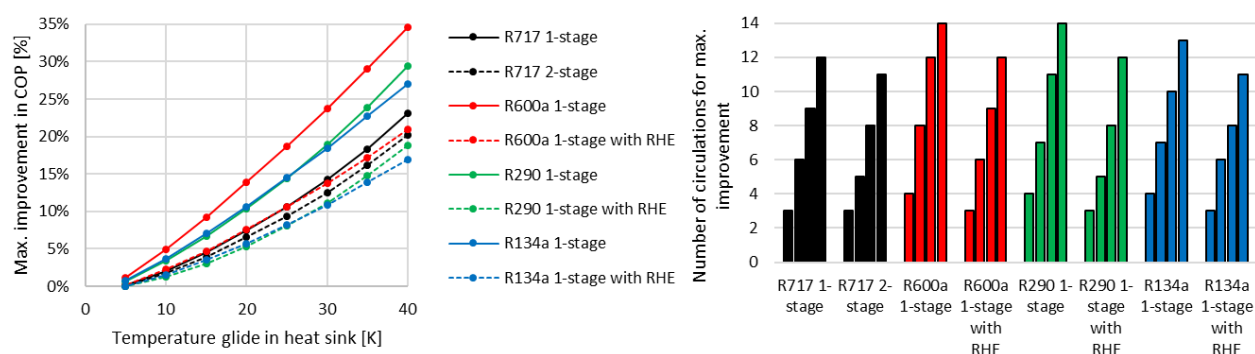


Figure 8: Left: Improvement in COP for varying temperature glide in heat sink. Right: Number of circulations with maximum COP for temperature glides of 10, 20, 30 and 40 K.

Figure 8, right, shows the optimum number of circulations per charging cycle for temperature glides of 10 K to 40 K in steps of 10 K. The fourth column of each working fluid and HP configuration shows the location of the maximum in Figure 8, left. It may be seen that the location of the maximum moves to lower numbers of circulations for decreasing temperature glides.

### 3.2.2.4. Temperature lift

The final screening investigates the influence of the temperature lift on the performance of the novel HP system. Figure 9, left, shows the maximum improvement in COP for different temperature lifts of 20 K to 60 K. The results with a temperature lift of 40 K coincide with the data for a temperature glide in the heat sink of 20 K in Figure 9, left. The data for the one-stage HP with R717 are shown only for temperature lifts of 20 K to 40 K. For higher temperature lifts, the discharge temperature exceeds the maximum allowed temperature of 180 °C. The highest improvement in COP was found for a one-stage cycle with R290 at a temperature lift of 20 K with 17 %. For temperature lifts above 20 K, the biggest improvement is achieved with a one-stage with R600a.

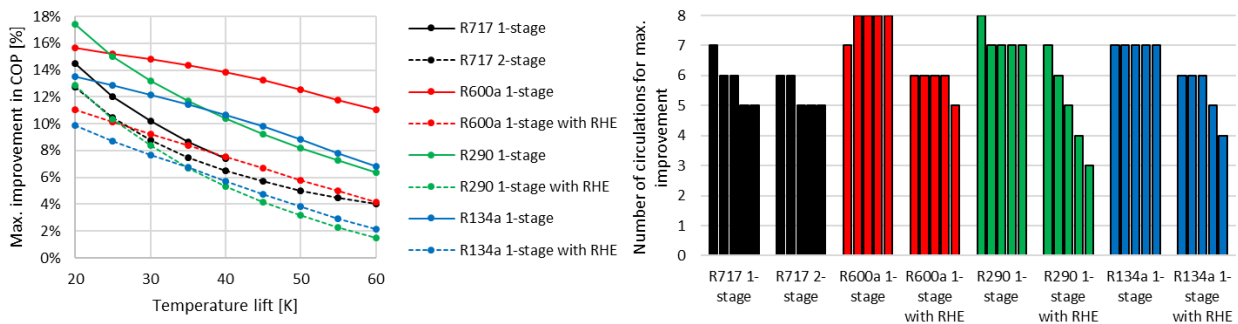


Figure 9: Left: Improvement in COP for varying temperature lifts. Right: Number of circulations with maximum COP for temperature lifts of 20, 30, 40, 50 and 60 K.

For all investigated cases, the increase in temperature lift leads to lower maximum improvement. However, the slope of the curves shown in Figure 9, left, differs between the cases. While the curves of R717 and R290 are steeper at lower temperature lifts for all HP configurations, they are close to linear for R600a and R134a in a one-stage HP with RHE, and for simple HPs they get steeper with increasing temperature lifts.

Figure 9, right, shows the location of the maximum for temperature lifts between 20 K to 60 K in steps of 10 K. It shows some differences between the cases. For a one-stage cycle with R600a, the number of circulations for the maximum improvement in COP increases with increasing temperature lifts. For a one-stage cycle with R134a, it remains constant at seven circulations, and for all other cases it decreases with increasing temperature lifts.

Figure 10 shows the COP at different temperature lifts of a one-stage and two-stage cycle with R717 for a conventional HP and the novel system using storage tanks. As in Figure 9, left, the data for the one-stage cycle are shown only for temperature lifts of 40 K or lower due to the limitations in the discharge temperature. As expected, all COPs decrease with increasing temperature lifts, and the COP of a conventional one-stage HP is lower than the one of a conventional two-stage HP. As seen in the previous screenings and also in Figure 9, left, the introduction of the tank system leads to a bigger improvement for the one-stage cycle than for the two-stage cycle. In this case, this leads to higher COPs for a one-stage configuration with storage tanks than for a conventional two-stage HP for temperature lifts below 35 K. For a temperature lift of 20 K, the COP of the one-stage cycle with tanks of 6.48 reaches almost the COP of the two-stage HP with tanks of 6.66.

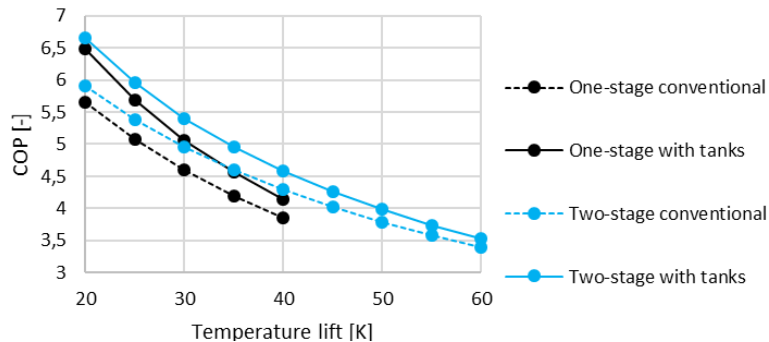


Figure 10: COP of one-stage and two-stage cycles with and without tank system with R717 for different temperature lifts.

### 3.2.3. Gradual heating and cooling

In this section, results for the evaluation of the performance of a heat pump system with gradual heating and cooling using the model introduced previously are shown. The study was presented at the 5th International Conference on Smart Energy Systems 2019 [14].

In this study, the simultaneous provision of district heating and cooling through gradual heating and cooling was investigated. For district heating, it was assumed that water is heated from 40 °C to 70 °C, while for gradual cooling, water is cooled from 15 °C to 8 °C. The study included an ammonia heat pump with a capacity of 300 kW and one with R600a of 10 kW. Both systems used a simple one-stage cycle. The performance of the two systems was examined by varying the number of circulations per charging cycle between 1 and 15 circulations. The number of circulations on the hot and the cold side was set equally. For the variation, the same design parameters as shown in Table 1 were used.

Figure 11 depicts how the COP of the system behaves for increasing numbers of circulations per charging. On the left side, the results for the case with R600a as working fluid are shown. It can be seen that with gradual heating and cooling, the maximum is reached at 6 circulations per charging, while for gradual heating only, it is reached at 15 circulations. The earlier peak of the COP for gradual heating and cooling derives from the water mass flow in the evaporator increasing with increasing number of circulations and the increased pressure drop connected with this. The same can be seen in Figure 11, right, for ammonia.

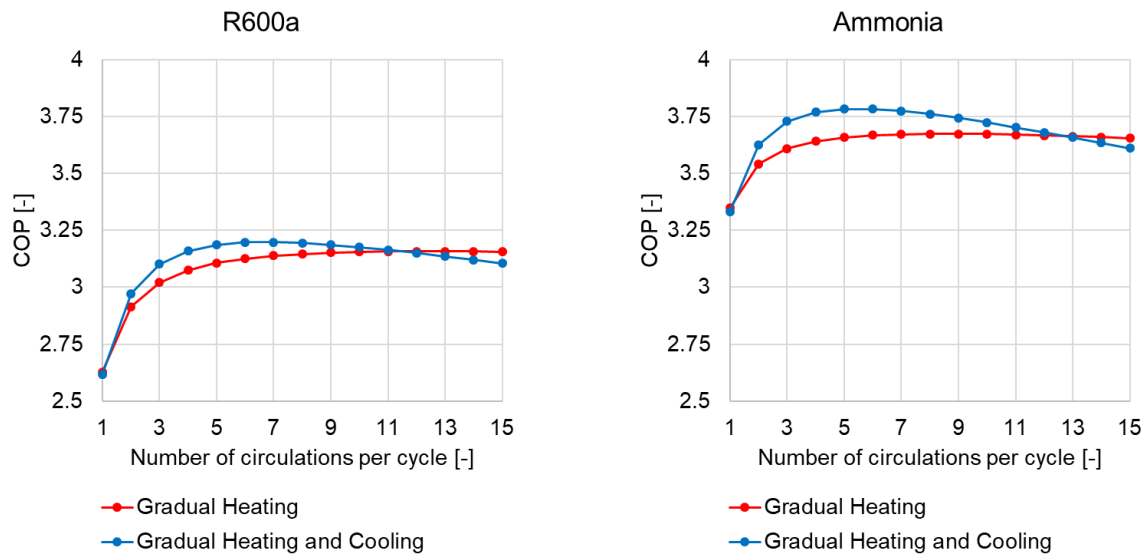


Figure 11: Left: Improvement in COP through gradual heating and gradual heating and cooling of one-stage cycle with R600a. Right: Improvement in COP through gradual heating and gradual heating and cooling of one-stage cycle with Ammonia.

It can also be seen that the maximum COP for both working fluids was achieved through gradual heating and cooling. Figure 12 shows the numerical results for the maximum achievable COP for a conventional heat pump, gradual heating and gradual heating and cooling for R 600a (left) and ammonia (right). The COP for the conventional heat pump corresponds to the value of  $N=1$  in Figure 11. In Figure 12, right, it is shown that the highest COP can be achieved by gradual heating and cooling with ammonia as working fluid with 3.78. However, compared to the conventional heat pump, the improvement of COP is on 13.6 %. When using R600a, the improvement is significantly higher with 22.2% for gradual heating compared to a conventional heat pump. On the other hand, the difference between gradual heating and gradual heating and cooling is larger for ammonia than for R600a.

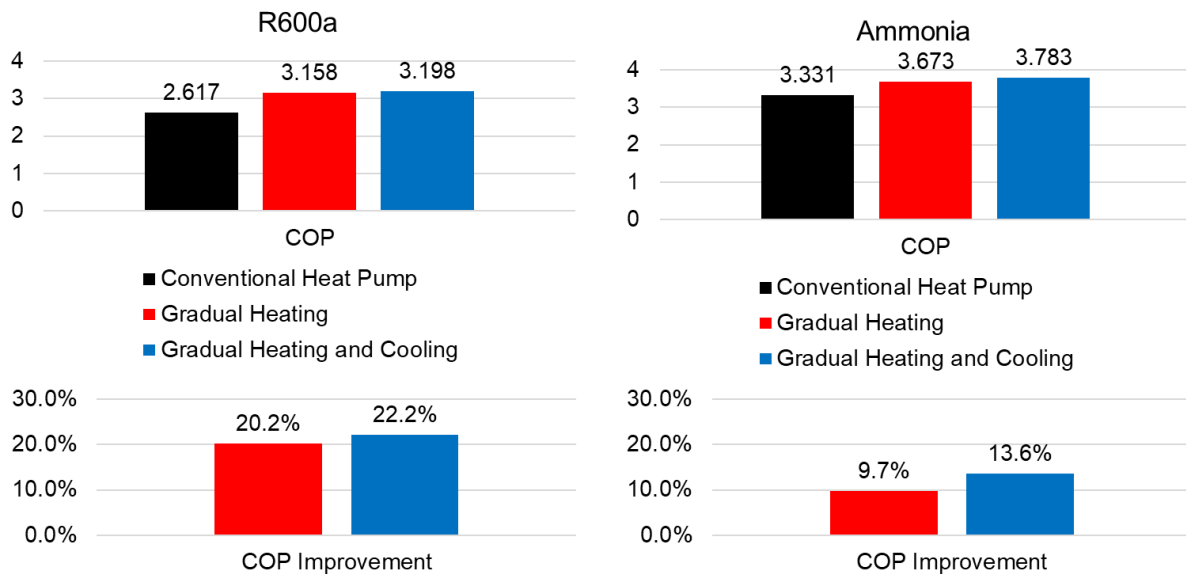


Figure 12: Left: Comparison of maximum COP of the different heat pump systems with R600a. Right: Comparison of maximum COP of the different heat pump systems with ammonia.

### 3.3. Dynamic modelling

In the quasi-steady-state models presented in section 1.2, the heat capacity of the equipment, the refrigerant and the water in pipes was not considered in the modelling. Varying the temperature set-points to obtain the gradual heating and cooling will in reality induce temperature gradients and transitioning periods, which are not captured by the quasi-steady-state models but may impact the performance of the system. In order to assess the impact of the heat capacity and valve switching, a dynamic model of the system with gradual heating was built.

#### 3.3.1. Dynamic model

Figure 13 shows the graphical representation of the dynamic system that was implemented using the Modelica language [15]. It is based on the TIL component library 3.4 [16] and was simulated using Dymola software [17]. The model consists of the three main parts:

- One-stage heat pump cycle with internal heat exchanger, using Isobutane (R600a) as refrigerant
- Source water flow
- Tank system on the sink side.

The heat pump cycle consists of a direct expansion evaporator, an internal heat exchanger that superheats the refrigerant in the suction line while subcooling the refrigerant in the liquid line, a reciprocating compressor, a desuperheater and condenser, a receiver downstream of the condenser, and an expansion valve that was used to control the superheat out of the evaporator. The sink side was modelled as a water flow at constant return temperature, where the mass flow rate was used to control the cooling supply temperature, i.e. the temperature of the exiting water stream from the evaporator. The needed pump and thus the pumping power have been neglected. On the sink side, the

proposed tank system was modelled. The return water from the process was again assumed to have a constant temperature. The tank system consists of a large storage tank and a smaller charging tank, as described above. Further, all water pipes, an expansion tank, a pump, and the necessary valves were included in the model. The valves were used to control the charging of the charging tank and in order to control the charging and discharging of the storage tank. The assumptions for the different components are given in the following.

### **3.3.1.1. Heat exchanger**

All heat exchangers, i.e. evaporator, condenser, and internal heat exchanger were modeled as plate heat exchangers that were discretized into finite volumes using the staggered grid approach. The condenser was split into two heat exchangers, namely the desuperheater and the condenser. It was assumed that the working fluid desuperheats in the first quarter of the heat exchanger and is condensed over the remaining length. The pressure loss was neglected in all heat exchangers. The heat transfer coefficients were assumed to be constant on the refrigerant side for the evaporator, condenser, and desuperheater. On the water side, the correlation by Martin [18] was used as well as in the internal heat exchanger. The heat transfer coefficients (and approaches) as well as the unknown plate geometries were fitted to the results from the Alfa Laval heat exchanger software [19] that was used to calculate and validate the behavior of the heat exchanger models in steady-state. The geometries and assumptions for all heat exchangers are summarized in Table 2.

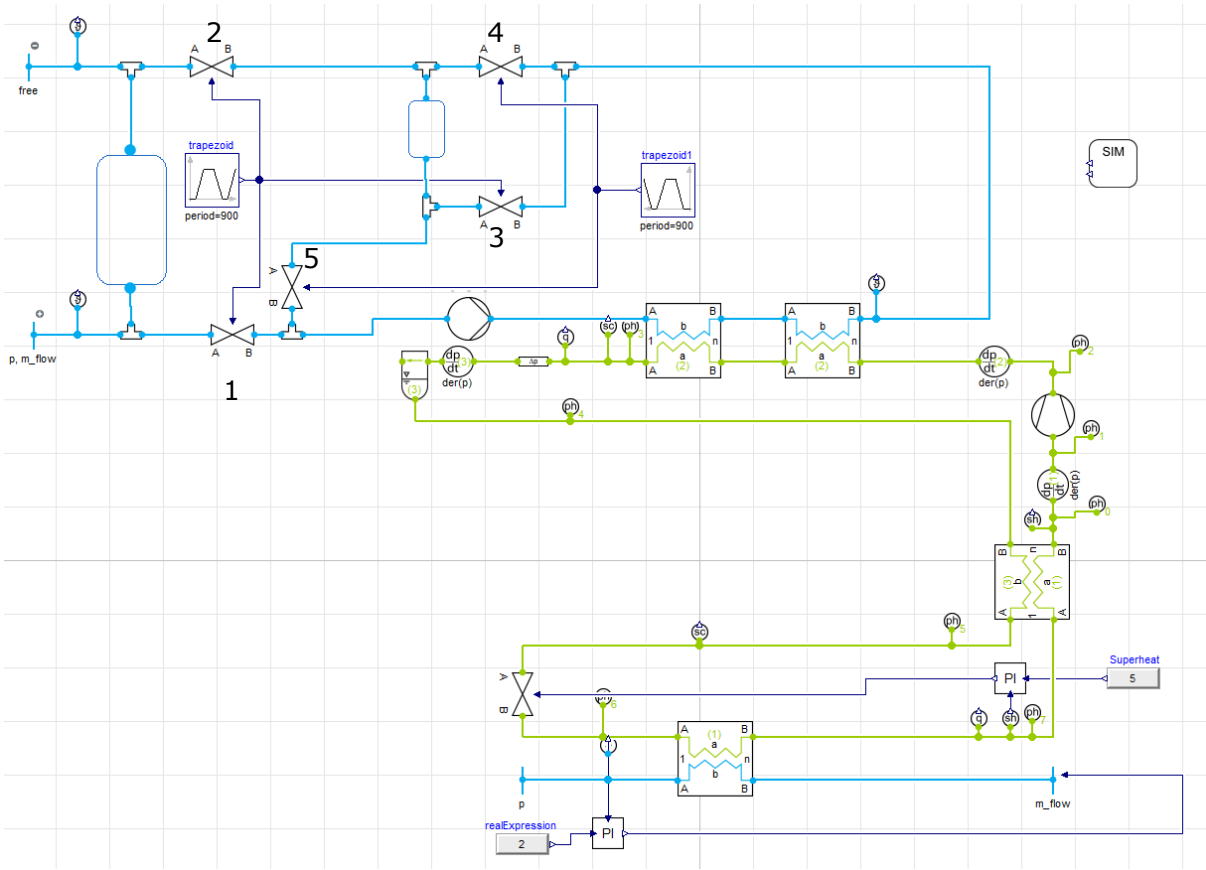


Figure 13: Graphical representation of the dynamic system that was implemented using the Modelica language.

### 3.3.1.2. Compressor

The compressor model was based on polynomials describing the volumetric and isentropic efficiency. The mass balance and energy balance were assumed to be quasi-steady, which is a common assumption for compressors since the dynamics are typically very fast compared to the dynamic response of heat exchangers and vessels in the system. These were fitted to data that was obtained from the compressor data base in PackCalc [13] for the Bock EX-HG 34P/315 4 compressor that was planned to be used in the real test rig. The following polynomials were used:

$$\eta_{is} = C[1] + C[2] * T_{evap} + C[3] * T_{cond} + C[4] * T_{evap}^2 + C[5] * T_{evap} * T_{cond} + C[6] * T_{cond}^2 + C[7] * T_{evap}^3 + C[8] * T_{evap}^2 * T_{cond} + C[9] * T_{evap} * T_{cond}^2 + C[10] * T_{cond}^3$$

With

$$C = [0.07379, -0.02024, 0.02712, -0.0001127, 0.0006757, -0.0004395, 2.236e - 6, -2.452e - 6, -5.266e - 6, 2.337e - 6]$$

$$\eta_{vol} = P[1] + P[2] * T_{evap} + P[3] * T_{cond} + P[4] * T_{evap}^2 + P[5] * T_{evap} * T_{cond} + P[6] * T_{cond}^2 + P[7] * T_{evap}^3 + P[8] * T_{evap}^2 * T_{cond} + P[9] * T_{evap} * T_{cond}^2 + P[10] * T_{cond}^3$$

With

$$P = [1.02, 0.0041, -0.004779, -1.356e - 5, -2.262e - 5, -1.286e - 5, 1.037e - 6, -3.083e - 6, 9.375e - 7, 9.193e - 8]$$

Table 2: Summary of heat exchanger specifications \*[18]

	Evaporator	Desuperheater	Condenser	IHX
Heat exchanger model	AC70X-30M	CBH62-20H	CBH65-20H	CBH30-14H
Number of Plates	30	20	20	14
Length	0.466	0.119	0.357	0.25
Width	0.111	0.113	0.113	0.113
Chevron angle	61	70	70	40
Wall thickness	0.0007	0.00065	0.00065	0.0008
Pattern amplitude	0.00075	0.0007	0.0007	0.00072
Pattern wavelength	0.012	0.00587	0.00587	0.12
Pressure loss VLE	Zero pressure loss	Zero pressure loss	Zero pressure loss	Zero pressure loss
Heat transfer coefficient VLE	Constant alpha =2900 Wm <sup>-2</sup> K <sup>-1</sup>	Constant alpha =370 Wm <sup>-2</sup> K <sup>-1</sup>	Constant alpha =3450 Wm <sup>-2</sup> K <sup>-1</sup>	Martin*
Pressure loss Liquid	Martin*	Martin*	Martin*	Martin*
Heat transfer coefficient Liquid	Martin*	Martin*	Martin*	Martin*
Wall material	Stainless steel	Stainless steel	Stainless steel	Stainless steel

### 3.3.1.3. Receiver

The receiver was modelled as an ideal separator, assuming equilibrium between the liquid and vapor phases. The volume was assumed to be 10 l as in the planned test setup.

### 3.3.1.4. Valves

All valves were assumed to have an adjustable opening degree. In the model, the cross sectional area may be set, thereby enabling to use the valves for control purposes. The mass flow rate through the valve was calculated using Bernoulli's equations, thereby representing the relation between the pressure drop across the valve and the mass flow rate through the valve.

### 3.3.1.5. Water tank models

The water tank models were discretized into 100 layers along the height of the tank. This was done in order to be able to represent the stratification within the tank. Buoyancy was neglected in order to keep the model numerically stable. Instead it was assumed that the content of two adjacent cells was mixed with a certain mixing factor (between 0 and 1,

where 0 means no mixing and 1 means complete mixing of the two control volumes) in order to model that warmer water in lower cells would move upwards due to the difference in density. This approach has been presented by [4]. For each control volume in the water tank, a dynamic mass and energy balance was solved and heat transfer across the tank shell, i.e. heat loss to the environment and to adjacent cells, was considered. The difference in hydrostatic pressure across the tank was neglected.

### **3.3.1.6. Pipes**

Within the tank system, pipes between every component were considered. All pipes were assumed with a length of 2 meters. Each pipe was discretized into 10 finite volumes.

### **3.3.1.7. Pump**

The water pump was modelled as a quasi-static component, assuming a constant isentropic efficiency of 0.8 and a fixed mass flow rate. The latter depended on the number of charging cycles.

### **3.3.1.8. Control strategy of the tank system**

For the tank system, a simple control strategy was implemented, which does not include any measurements within the system. The valve position was set to discharge the charging tank for 300 seconds at the end of each charging cycle, by opening the valves 1, 2 and 3 and closing the valves 4 and 5 in Figure 13. Afterwards, valves 1, 2 and 3 were closed and valves 4 and 5 were opened for  $(N-1)*300$  seconds, in which the gradual heating is conducted, while the processes are fed from the storage tank.

### **3.3.1.9. Investigated case study**

With the dynamic model, a case study based on the available data on the examined test rig of the project was conducted. The one-stage cycle with internal heat exchanger and R600a as working fluid was used to provide cooling at a constant temperature of 2 °C with a return temperature of 6 °C. It was assumed that the cooling is flexible to varying mass flows, as a buffer tank should be used. The condenser is connected to the tank system, from which district heating is provided. The return temperature from the district heating was assumed to be constant at 40 °C. The heat pump was modelled with the original components of the test rig information available, as explained in the previous sections. The compressor was assumed to run a constant, maximum speed of 1450 RPM. The forward temperature to the district heating grid is then a result of the operation of the heat pump, the mass flows in the tank system, and the control of the cold forward temperature. The size of the storage tank was kept constant, while the size of the charging tank was increased with increasing number of circulations per charging cycle. The sizes were determined using the quasi-steady-state model presented in section 3.2.1.

## **3.3.2. Results**

Firstly, the dynamic model was used to assess the start-up of the system. The storage tank and the charging tank started with a uniform temperature of 40 °C. For all investigated cases, it takes roughly 10 to 12 hours until the supply temperatures to the process stabilize. This is mainly caused by the necessity of warming up the water in the storage

tank. The larger size of the storage tank compared to the charging tank leads to having a significant amount of cold water (40 °C) remaining in the tank which is slowly warmed up, while cooling down the warm water on top through heat conduction in the thermocline and through the tank walls.

In order to evaluate the performance of the system including the dynamic behavior of the system, it was simulated for 12 hours, and the COP was calculated for the last charging cycle of the simulated period. Figure 14 shows the COP calculated with the quasi-steady-state model in black and including the dynamic behavior in blue for up to nine circulations per charging cycle. We can see that the improvement in COP is reduced significantly, when including the dynamics. The ideal system, assuming no heat transfer or mixing in the tanks and a steady-state heat pump, predict an improvement from 3.15 to 3.31. The dynamic behavior of the system reduced this improvement to reaching a maximum of 3.17.

There are several factors influencing the shown differences. Firstly, the results showed that the assumption of a constant water pressure drop in the condenser for different numbers of circulations per charging cycle is not accurate. The pressure drop increases with increasing circulations as the mass flow increases while using the same heat exchanger. The increased pressure drop leads to a higher power consumption at higher numbers of circulation, causing a drop in COP. A second reason for the drop at higher number of circulations is the fact that the sizes of the storage and charging tank approach with higher number of circulations. This leads to having more hot water in relation to cold water in the storage tank. The heat transfer in the storage tank leads to some of the heat reaching the bottom of the tank. Hence, the inlet temperature to the condenser in the first circulation increases (>40 °C), leading to a higher temperature lift between the source and heat sink and subsequently to a lower COP of the system.

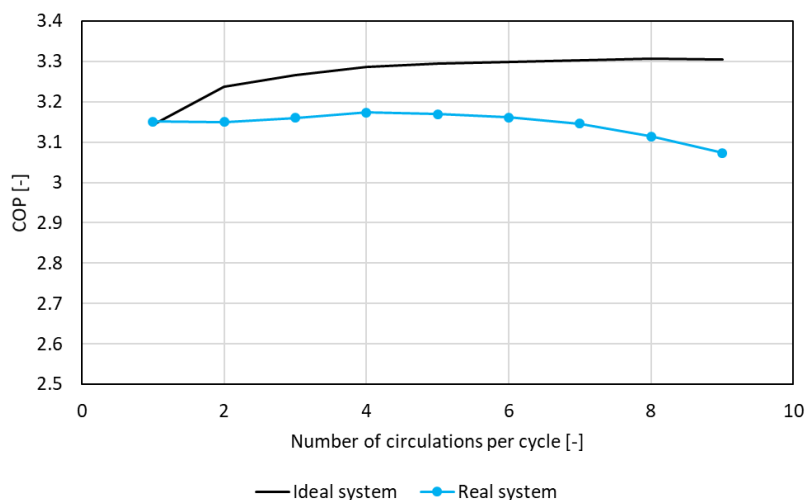


Figure 14: Comparison of real COP of the dynamic system compared to idealized calculation using the quasi-steady-state approach.

These two factors explain the strong decline at high numbers of circulations per charging cycle compared to the ideal system. The general difference between the two curves derives from the inertia, heat transfer and mixing in the tank system and the dynamics in the heat pump. Figure 15 depicts the condensation pressure as assumed in the quasi-steady-state approach compared with the dynamic behavior for the case of three circulations pre charging cycle.

At the beginning of the charging cycle, it can be seen that the condensation pressure does not immediately decrease to the pressure of the first circulation, but it takes more than 100 seconds to reach it. This is caused by two factors.

Firstly, the valves in the tank system take some time to close/open. In this case, the switching time was 15 seconds. A parameter variation showed that reducing the valve speed to 1 second does not improve the system. However, increasing it to 30 seconds negatively affects the system performance by further slowing the decrease of the condensation pressure. Secondly, the pipes in the water loop induce some inertia in the system, leading to the inlet temperature to the condenser not jumping directly from a high to a low temperature but decreasing gradually. Lastly, the dynamic behavior of the heat pump additionally slows the decrease of the condensation pressure. This mainly derives from the use of the internal heat exchanger. The internal heat exchanger leads to having relatively constant inlet conditions to the expansion valve, which is used to control the superheating but at the same time significantly influencing the condensation pressure. The small changes in inlet conditions to the expansion valve lead to very small changes in superheating and hence to a slow change in the expansion valve. This leads to a slow reaction of the condensation pressure to the changes in the inlet water temperatures in the condenser. It can be assumed that a heat pump without internal heat exchanger would react faster. However, the results showed that the internal heat exchanger ensures that vapor is entering the compressor, while the outlet of the evaporator is usually not fully evaporated for some seconds after the jump in condenser inlet temperatures. This would lead to damaging the compressor and inhibiting safe operation of the system. Additionally, for heat pumps running with R600a, the removal of the internal heat exchanger would reduce the COP, as shown in section 3.2.2.2.

After reaching a constant condensation pressure, it is seen that the steps in condensation pressure are actually not steps, but the pressure increases slowly. This derives from the heat transfer between the different layers in the charging tank, leading to a slow increase in the inlet temperature to the condenser instead of a step. Additionally, the slow reaction of the heat pump further influences the behavior.

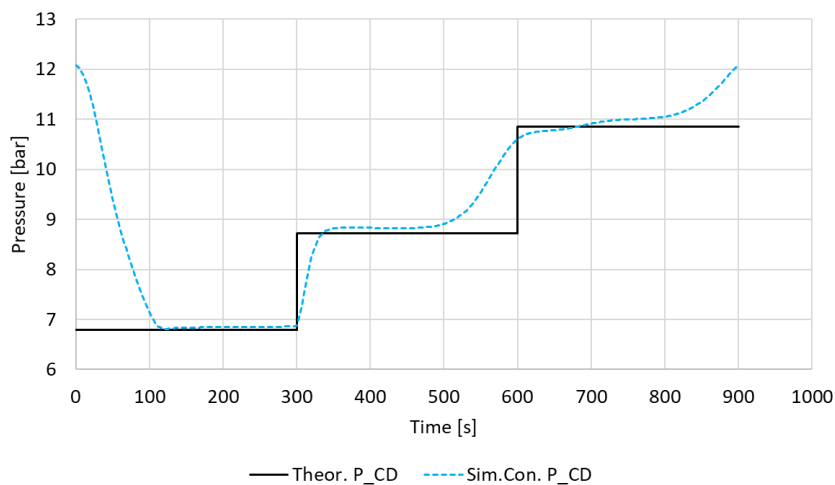


Figure 15: Dynamic behaviour of condensation pressure compared to the ideal behaviour assumed for quasi-steady-state calculations. The time period shows the behaviour for the last circulation after 12 hours of operation.

In order to assess the influence of the dynamics of tank system and heat pump on the performance of the system separately, additional simulations were conducted. The simulations included:

- A system with the real tank system including all the components of the dynamic model and a steady state heat pump, where the heat output and COP are only dependent on the water inlet temperature to the condenser (System 2).
- A system with the real heat pump including all the components and controllers of the dynamic model and an idealized tank system without inertia, heat transfer, and mixing, supplying always the same temperatures that were put into the tank (System 3).

Table 3 compares the heat pump COP and the system COP of the different systems for three circulations per charging cycle and for a conventional heat pump without tank system. The heat pump COP (COP\_HP) denotes the cumulative heat output of the heat pump over the cumulative power input of the compressor and the pump. The system COP (COP\_Sys) denotes the cumulative heat output of the system to the process over the cumulative power input of the compressor and the pump. The difference between the two values describes the losses in the tank system.

The results show that both the tank system and the heat pump have an influence on the performance. It can be seen that assuming an ideal tank system in systems 1 and 3 leads to having the same system COP as heat pump COP, as there are no losses in the tank system. On the other hand, in system 2 it can be seen that having a real tank system does not only reduce the tank efficiency but also reduces the heat pump efficiency. Overall, the results show that the influence of the tank system and the heat pump are similar, and the cumulative impact reduces the COP significantly, reducing the COP from 3.30 (System 1) to 3.13 (System 4), which is lower than the COP of a conventional heat pump without tank system with 3.15 (System 5).

*Table 3: Heat pump COP and system COP of heat pump system with gradual heating, including or neglecting the dynamic behaviour of part of the system. System 1-4 were calculated for three circulations per charging cycle*

<b>System No.</b>	<b>System definition</b>	<b>COP_HP</b>	<b>COP_Sys</b>
1	Ideal system	3.30	3.30
2	Tank dynamic, HP ideal	3.26	3.20
3	Tank ideal, HP dynamic	3.22	3.22
4	Fully dynamic system	3.19	3.13
5	Conventional HP	3.15	3.15

When evaluating the results shown in Table 3 it should be considered that systems 1, 2 and 3 are technically not feasible, as the laws of physics cannot be avoided. System 2 is the system that can be approximated technically, as all the losses in the tank system are physical, while the heat pump control could theoretically be improved to approach the ideal behavior.

Considering this it should be noted that the theoretical improvement potential of the COP is reduced from 4.8 % (System 1 versus System 5) to 1.6 % (System 2 versus System 5).

It should be noted that the absolute values and results strongly depend on the heat pump and tank system layout, the refrigerant, and the used components in the system. However, including the dynamics in the simulation of the system will always lead to lower performances than the quasi-steady-state approach.

### 3.4. Summary

This part conducted at DTU Mechanical Engineering covered the thermodynamic evaluation of the whole system. This was done by building two different models.

The quasi-steady-state model was built for fast and robust calculation of the improvement potential of the COP of a heat pump system through addition of a tank system on the hot side or on the hot and the cold side. The model enables to examine the improvement potential for different heat pump configurations, tank system layouts, refrigerants, sizes of heat exchangers, and different types of compressors. The user can vary the boundary conditions using a graphical user interface, enabling the investigation of any physically reasonable case.

The model was used to examine the influence of different parameters on the improvement potential by gradual heating compared to a conventional heat pump. The study included the influence of the choice of heat pump configuration and refrigerant, and variations in the temperature lift and temperature glide. The study showed that the improvement potential is highest for simple heat pump configurations and with R600a as refrigerant. Increasing temperature glides in the heat sink and decreasing temperature lifts between source and sink increase the improvement potential. Additionally, we used the model to conduct a study on the improvement potential in COP through gradual heating and cooling for providing district heating and district cooling at the same time. The study included two heat pumps with R600a and ammonia as refrigerants, respectively. The study showed that also for gradual heating and cooling, higher improvement can be achieved using R600a. However, when comparing the difference between gradual heating only and gradual heating and cooling, a larger increase in COP was found for ammonia.

In a second step, a dynamic model of the system was built. The system layout and component sizes were chosen according to the available information of the planned test setup. The sizing of the charging tank and the control was done using the quasi-steady-state model. The results showed that the assumptions of neglecting the heat pump dynamics and the heat transfer, mixing and dynamics in the tank system in the quasi-steady-state model lead to an overestimation of the improvements in COP. Examining the influence of the dynamics in the tank system and the heat pump separately showed that both phenomena have a similar impact on the lower COP. The negative influence of the heat pump dynamics could possibly be reduced through changing configuration or advanced control. The influence of mixing and heat transfer in the tank system are physical phenomena and can therefore not be neglected. This leads to the conclusion that the quasi-steady-state model is suited for getting an idea of whether an improvement in COP is possible and it can help to design the tank sizes, but it should be considered that the predicted COP improvement will be smaller due to the dynamic behavior of the system.

## 4. Effect of tank design on COP

### 4.1. Introduction

This investigation was done as a part of the ISECOP project, where a heat pump was used for heating and cooling two storage tanks simultaneously, as it is presented in Figure 16. The part of the system investigated using Computational fluid Dynamics (CFD) is the one marked with a red square in Figure 16. In order to make the modelling easier, the hot and the cold side of the heat pump were individually simulated, following the same methodology presented below. The objective of this project was to examine the effect of the tank design on the COP of the tank heat pump system during charge and discharge. Parameters such as the tank geometry, flow rate, diffuser plate geometry and tank material were investigated using CFD, in order to determine the effect of these parameters on the final performance of the system.

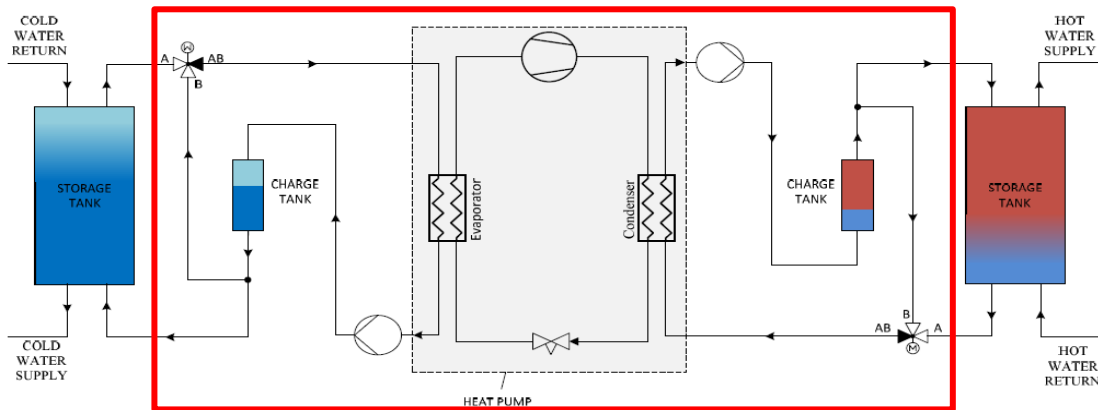


Figure 16: The ISECOP concept. CFD-calculations used for the part in the red square.

#### Nomenclature

$d$	Diameter [m]
$h$	Height [m]
$m_{\text{steel}}$	Mass of steel [kg]
$m_{\text{water}}$	Mass of water [kg]
$C_{p\text{steel}}$	Specific heat capacity of steel [kJ/(kg K)]
$C_{p\text{water}}$	Specific heat capacity of water [kJ/(kg K)]
$T_{\text{initial, steel}}$	Average temperature of tank's steel at start of charge operation [K]
$T_{\text{final, steel}}$	Average temperature of tank's steel at end of charge operation [K]
$T_{\text{initial, water}}$	Average temperature of tank's water at start of charge operation [K]
$T_{\text{final, water}}$	Average temperature of tank's water at end of charge operation [K]

$Q$	Amount of heat stored in tank [kJ]
$V$	Volume [L]
$\rho$	Water density [kg/m <sup>3</sup> ]
$Q_c$	Heat output from the condenser [kJ]
$W$	Power consumption of compressor [kJ]

#### Abbreviations

COP	Coefficient Of Performance
CFD	Computational Fluid Dynamics
UDF	User Defined Function

## 4.2. Methodology

The investigated system consists of an 8.9 kW heat pump connected to a 109.6 L vertical cylindrical storage tank. The fluid used in this heating system was water. The tanks used were made of steel with a wall thickness of 2.5 mm at the sides of the tank and a wall thickness of 3 mm at the top and the bottom of the tank. Since the heat pump's characteristics were known, calculations were performed and the temperature increase of water passing through the heat pump was determined for a given volume flow rate. It was assumed that the inlet temperature of the heat pump was equal to the outlet temperature of the tank and that the outlet temperature from the heat pump was equal to the inlet temperature of the tank. That way, water from the tank outlet would pass through the heat pump and, after being heated up (or cooled down), it would return to the inlet of the tank without having in principle any thermal losses from the pipes. Figure 17 shows the inlet temperature of the tank as a function of the outlet temperature of the tank based on heat pump operation.

A User Defined Function (UDF) was written in ANSYS Fluent in order to create the temperature profile for the inlet of the tank. The UDF found the area averaged temperature at the outlet of the tank and then increased it based on the curve presented in Figure 17. Afterwards, the UDF applied the obtained temperature to the inlet of the tank. The temperature range of the charge operation was from 35 °C to 75.3 °C. For the discharge operation, cold water of 35 °C was supplied at the bottom of the tank, and hot water located at the top of the tank was discharged. The temperature range of the discharge operation was from 75.3 °C to 60 °C.

In order to make a fair comparison between the various solutions tested, a control method was developed, which stopped the simulation (either the charge or the discharge) when the temperature at the inlet/ outlet of the tank reached a specific value. The control set-point temperatures were 75.3 °C and 60 °C for the charge and the discharge, respectively. In this way, the energy content of the tanks at the end of the charge/ discharge was almost the same and it was mainly affected by the heat transfer between the water and the tank wall and by mixing. Therefore, the charge/discharge duration of the tested solutions was not exactly the same.

The investigated parameters were:

- Tank dimensions (variations in the height/diameter ratio)
- Diffuser designs
- Tank wall material (scenario with a hypothetical material having zero specific heat capacity and thermal conductivity – meaning no heat transfer between the water and the tank wall, no possibility to store heat in the tank walls, no heat loss, and no downwards heat transfer through the tank walls).

The same methodology was used for the tank located on the cold side of the heat pump.

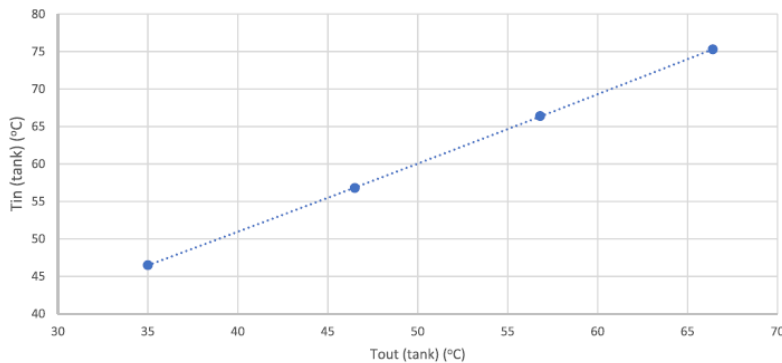


Figure 17: Correlation between the tank's inlet and outlet temperature based on heat pump operation for "small tanks hot side".

### 4.3. COP calculation

In order to evaluate the performance of each system under investigation, two different COP expressions were developed: COP during charge and COP during one full cycle of operation (charge and discharge):

COP during charge:

$COP_1 = \text{Total heat in the tank by end of charge} / \text{Total electricity consumption for heat pump}$

COP for charge and discharge:

$COP_2 = \text{Total tapped energy} / \text{Total electricity consumption for heat pump}$

Where the "heat in the tank by end of charge" is calculated by the equation:

$$Q = [m \cdot C_p \cdot (T_{final} - T_{initial})]_{\text{water}} + [m \cdot C_p \cdot (T_{final} - T_{initial})]_{\text{steel}}$$

The "total tapped energy" is the energy removed from the tank during discharge:

$$Q = \rho \cdot C_p \cdot \Delta T \cdot V$$

The "total electricity consumption" is calculated using the COP equation:

$$COP = Q_c / W$$

Where  $\Delta T$  is the average difference between inlet and outlet temperature of water and V is the volume of tapped water.

### 4.4. Small tanks hot side

The initial diffuser design for the tank was a two-plate diffuser as it can be seen in Figure 18. However, some initial investigations indicated that a 2-plate diffuser created a "dead volume" between the bottom plate of the diffuser and the tank. For this reason, it was decided to investigate single plate diffuser designs in order to utilize the entire tank volume. In addition, it was noticed that if the distance between the top plate of the diffuser and the inlet was increased, a larger mixing region inside the tank was created. This can be observed in Figure 18, where the velocity vectors inside the tank are presented for a 2-plate diffuser having different distances between the plates.

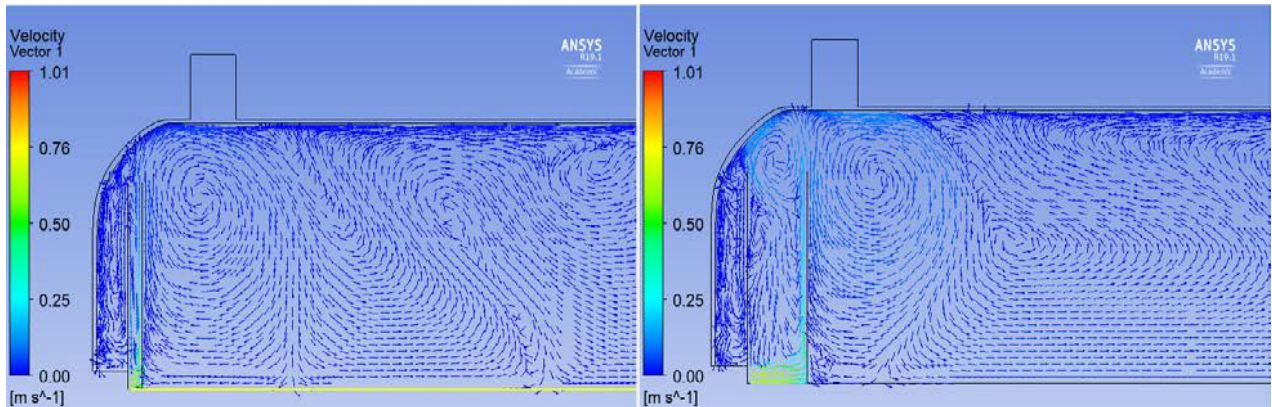


Figure 18: Velocity vector profiles for 2-plate diffusers of 13 cm radius having a distance of (a, left figure) 1 cm and (b, right figure) 4 cm.

Based on the initially obtained results, it was decided to investigate four different diffuser scenarios, which are presented in Table 4. A schematic of the investigated diffusers is presented in Figure 19.

Table 4: Tested tank diffusers

	Scenario A	Scenario B	Scenario C	Scenario D
<b>Description</b>	No diffuser present inside the tank	Single plate diffuser (large)	Single plate diffuser (small)	Perforated single plate diffuser having the same diameter as the tank
<b>Distance from inlet/outlet[m]</b>	-	0.01	0.01	0.01
<b><math>d_{diffuser}/d_{tank}</math></b>		-	0.73	0.3
<b><math>d_{pipe\ inlet/outlet}</math> [m]</b>	0.022	0.022	0.022	0.022

“Scenario D” had a 2 mm thick plate with a porosity of 5 %, corresponding to 66 holes of a diameter of 0.0075 m spread uniformly over the plate area. It also has to be stated that “Scenario D” had a small nonperforated cyclic region with a diameter of 0.044 m in front of the inlet, in order to block the direct inlet of water jet in the tank. The red area in Figure 19 (c) represents the perforated part of the “Scenario D” plate, which had an outer diameter of 0.276 m.

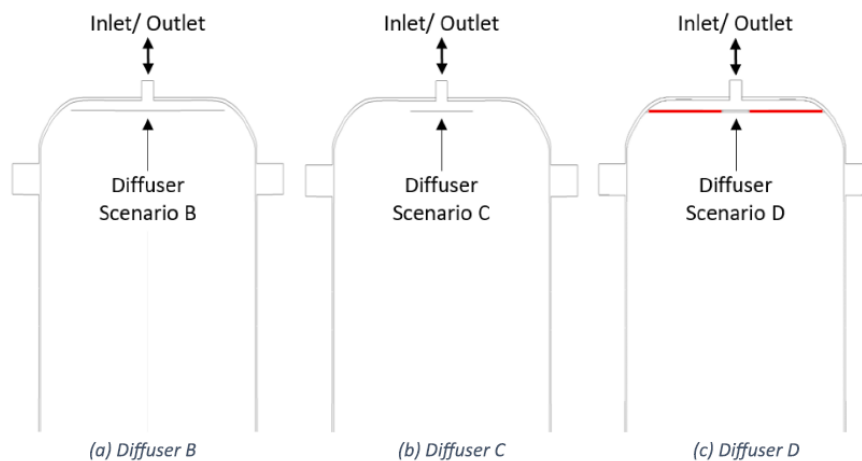


Figure 19: Diffuser designs mounted on the tank top.

These diffusers were mounted in three different tank designs, which had different height to diameter ratios. The dimensions of the tanks are presented in Table 5.

Table 5: Investigated tank dimensions

Parameter	Tank 1	Tank 2	Tank 3
Height to diameter ratio, h/d [-]	3.64	2	1
Height, h [m]	1.25	0.82	0.52
Diameter, d [m]	0.34	0.41	0.52
Tank volume, V [L]	109,6	109.6	109.6

Two different charge and discharge modes were investigated. The difference between the two modes was the flow rate in the tank loop and consequently the duration of the charge and discharge operation. Mode 1 had a flow rate of 0.24 kg/s and Mode 2 had a flow rate of 0.12 kg/s. In the results presented in this report, Mode 1 is referred as “high” case and Mode 2 as “low” case. These two flow rates were applied to all tested tank geometries.

In Figure 20 - 31, the results of the CFD simulations are presented by a number of curves. A theoretical ideal curve was drawn on each figure in order to compare each case with the ideal scenario. This curve shows how the figure would look like if there were no tank material, no thermal conduction, no heat loss, and no mixing inside the tank. The heat storage tank is heated up in 3 heating cycles. In each heating cycle, there is a temperature rise of approx. 9.4–11.5 K. The ideal curve for charge has a staircase shape because the ideal tank has a uniform temperature and perfect thermal stratification in the tank. The tank will be heated up as plug flow in 3 steps. In a similar way, the ideal curve for discharge has a knee shape. Due to the heavy insulation of the tank ( $U=0.22$  [W/m<sup>2</sup> K]), heat loss of the tank is expected to have a minor impact on the results of the simulations. For this reason, it is deliberately not discussed in this report.

In Figure 20, the temperatures at the outlet of the tank during the charge operation can be seen. The “ideal case”, which has the highest degree of stratification, has a staircase shape. However, the result shows that none of the simulated cases were similar to the “ideal case”. This means that the obtained results were affected by mixing and thermal conduction. Comparing the simulation results, the effect of mixing can be easily spotted, since all investigated scenarios had similar thermal conduction effect. It can be seen that for the case without a diffuser (Tank 1A high), a high degree of mixing occurs inside the tank (relatively straight curve). On the contrary, the case having a perforated plate diffuser (Tank 1D high), had the most stratified temperature profile, getting the closest to the “ideal case”.

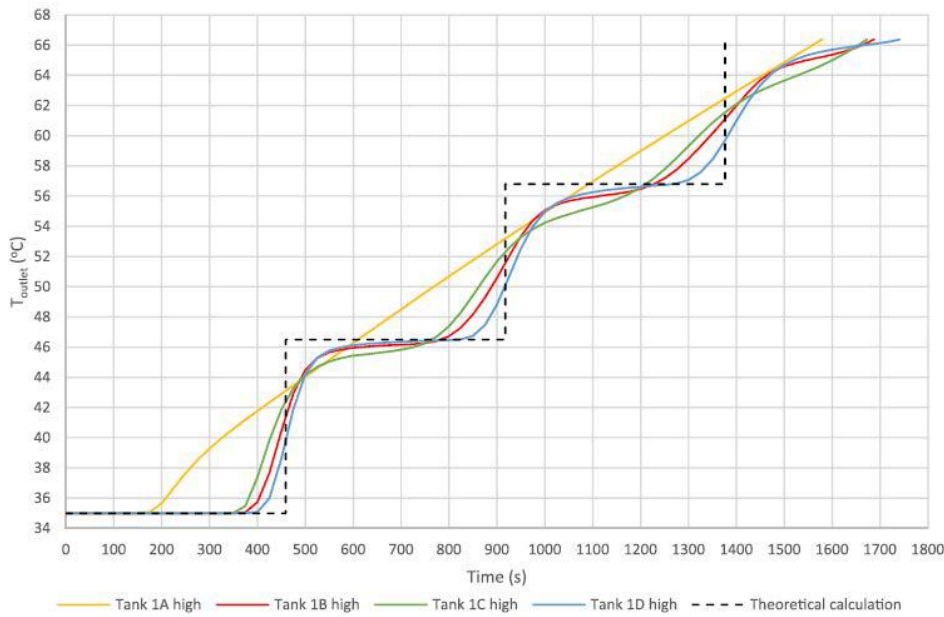


Figure 20: Average temperature at tank outlet during charge – high flow rate ( $h/d = 3.64$ ).

Figure 21 presents the tapped energy versus the outlet temperature during discharge operation. It can be observed that the simulation results are very different compared to the “ideal case”. The reason is that, in the “ideal case”, the whole tank has the same temperature during discharge due to the assumption that there is no vertical thermal conduction in the tank and no mixing with the low-temperature water entering in the bottom of the tank, whereas this is not the case in real-life situations. In addition, in the “ideal case”, since tank material is not considered, energy is not stored in the tank walls leading to a lower energy content compared to the simulated cases. It can be observed that in “Tank 1A high”, most of the tank’s volume has a temperature of 69 °C due to mixing, leading to a “knee” shaped curve. The case with the smallest amount of mixing, Tank 1D, was the one able to provide the highest tapped energy during discharge.

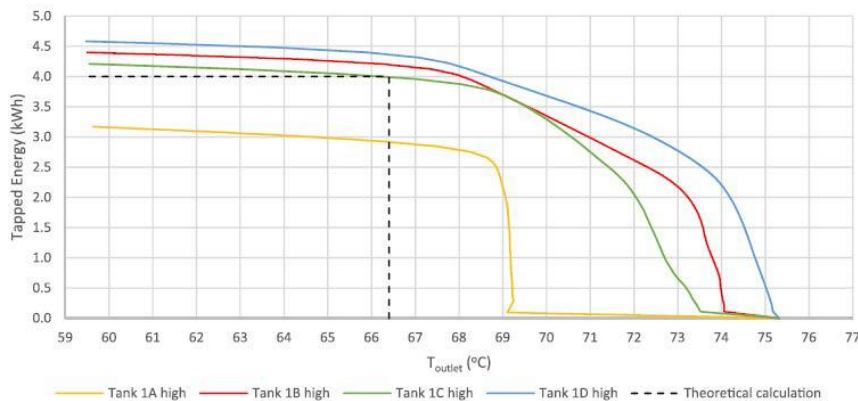


Figure 21: Tapped energy during discharge for a given outlet temperature – high flow rate ( $h/d = 3.64$ ).

Similar results were obtained for the low flow rate, as it can be seen in Figure 22 and Figure 23. The major difference was found for the tank without a diffuser (Tank 1A). It can be observed that for the low flow rate the curves “Tank 1A low”, for both charge and discharge,

came closer to the other diffuser results, unlike for the high flow rate, due to lower mixing. Since the effect of low flow rate on the results was only obvious for the tank without a diffuser (Tank 1A), it was decided not to present the low flow results for the other h/d tested, for space saving purposes.

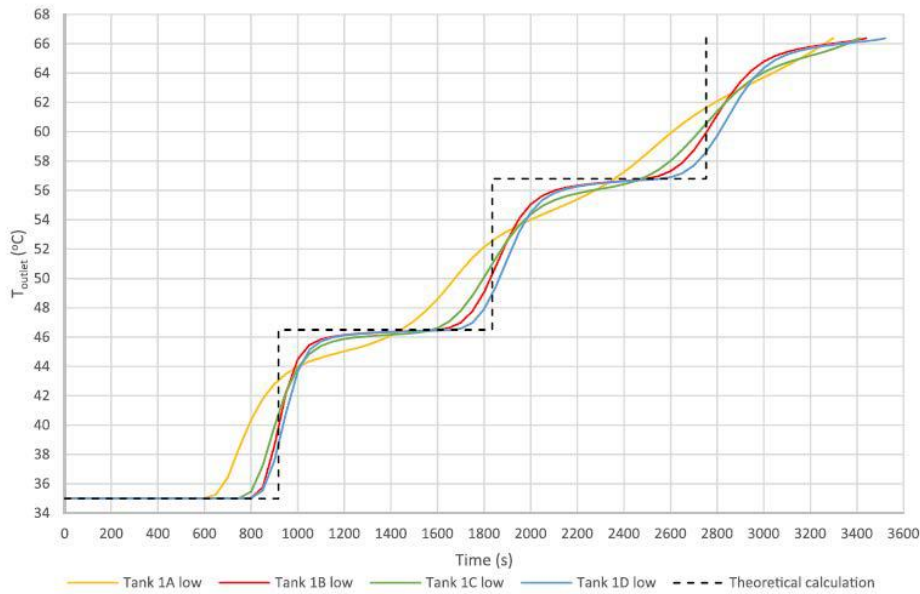


Figure 22: Average temperature at tank outlet during charge – low flow rate ( $h/d = 3.64$ ).

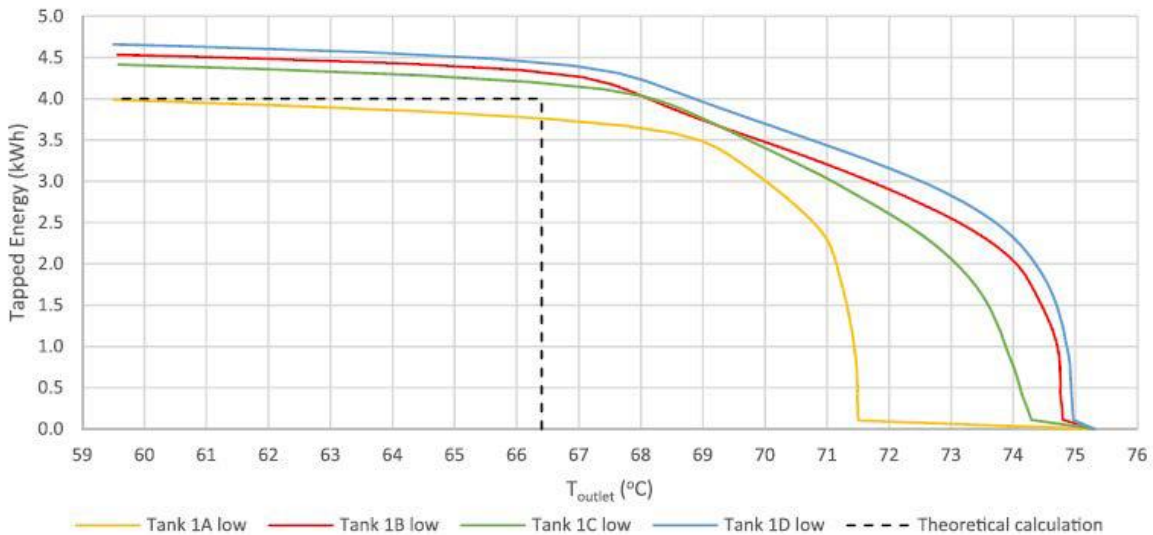


Figure 23: Tapped energy during discharge for a given outlet temperature – low flow rate ( $h/d = 3.64$ ).

The effect of the diffuser designs on the mixing in the tank is shown in Figure 24, where the velocity vectors close to the top of the tanks during charge are presented. “Tank 1A high” and “Tank 1C high” have a larger region of high velocities compared to the other two solutions where the high water velocities are limited close to the inlet. It can also be observed that water recirculation zones are developed in all cases except “Tank 1D high”. Finally, in all cases, the cooling of water close to the tank walls is visible, creating a

downflow of cooler water with relatively high velocity. Similar flow patterns were seen for the low flow cases but with relatively lower maximum velocity magnitudes.

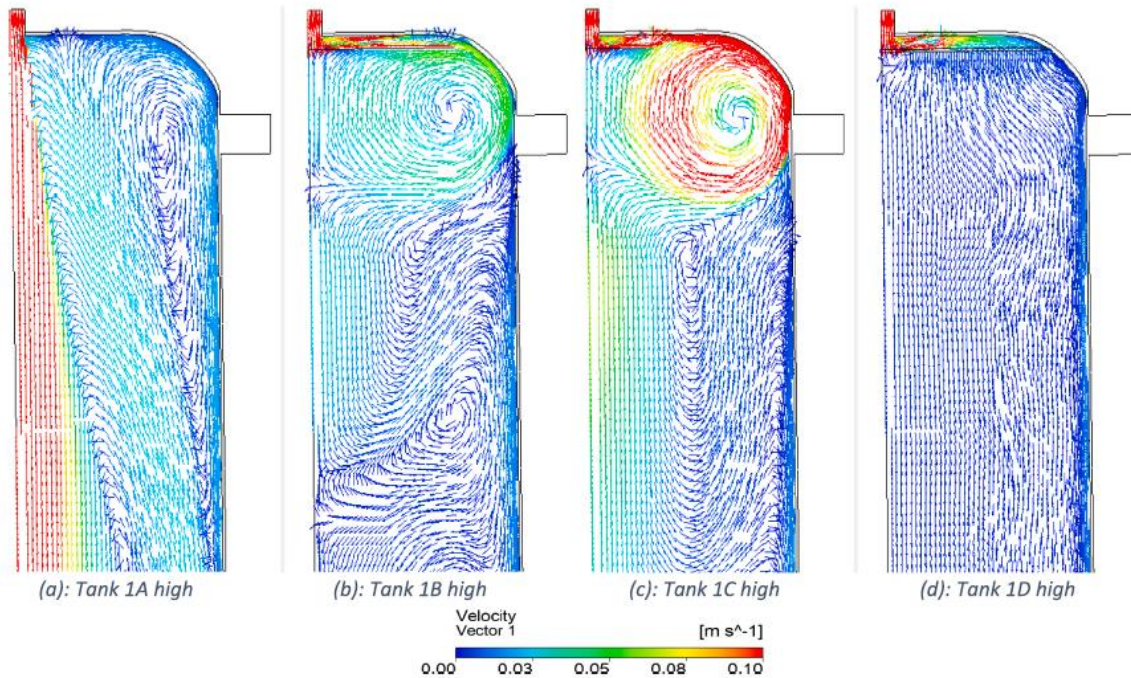


Figure 24: Velocity vectors at the top part of the tanks during charge (Tank 1,  $h/d=3.64$ ).

The velocity vectors shown in Figure 24 have a direct impact on the temperature contours inside the tank as it can be seen in Figure 25. The results show that the slim-tall tank is able to create thermal stratification in the tank in all cases, regardless of the amount of mixing, due to the high height to diameter ratio of the tank. This is obvious in Figure 25 (a) where, in spite of the high degree of mixing at the top of the tank, a relatively large temperature gradient is established at the bottom of the tank. Similar temperature contours were observed for low flow conditions.

The two COPs of the system were calculated and presented in Table 6. "Tank 1B high" has the highest  $COP_1$  and "Tank 1D high" and "Tank 1D low" have the highest  $COP_2$ . The reason of the difference is that  $COP_1$  only takes into account the temperature at the bottom of the tank but not the entire temperature profile inside the tank. This can also be seen in Figure 25 (a), (b) and (c), where although the tanks are thermally stratified in the bottom of the tank, the top of the tank is not stratified. This difference in the temperature profile affects  $COP_2$ ; therefore, it is more accurate to evaluate the performance of the system based on  $COP_2$ .

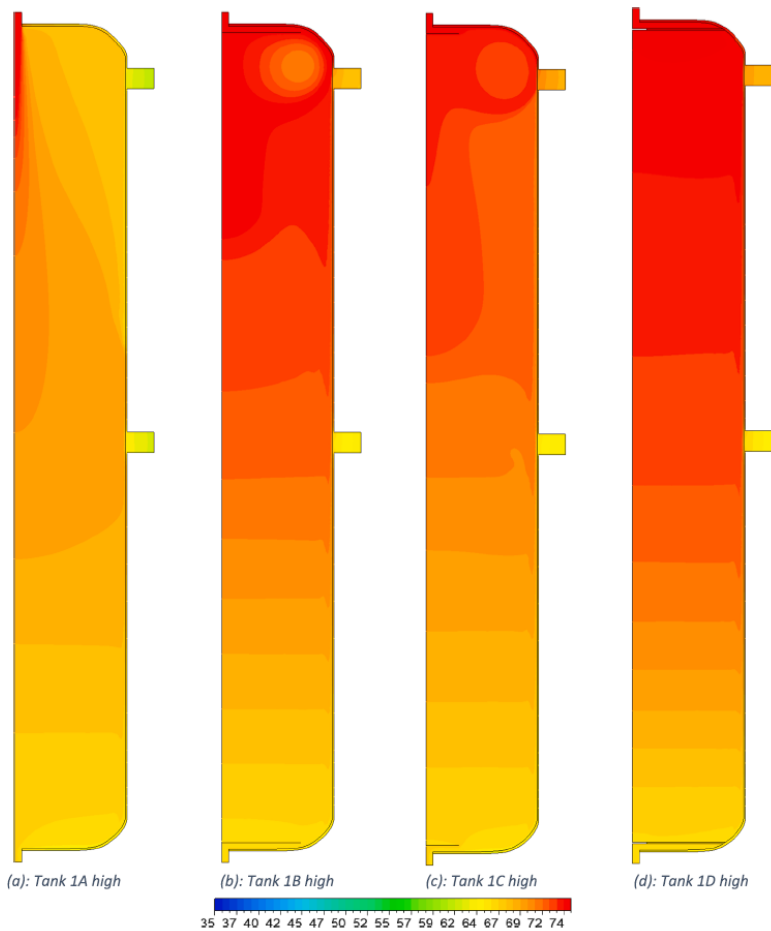


Figure 25: Temperature contours ( $^{\circ}\text{C}$ ) inside the tanks at the end of charge ( $h/d= 3.64$  tanks).

Generally, as it was expected since the tank is well-insulated, lower flow rates give higher  $\text{COP}_2$  due to a lower degree of mixing inside the tank. However, the highest  $\text{COP}_2$  was the same for "Tank 1D high" and "Tank 1D low" proving that when using a diffuser design that minimizes mixing, the results become less dependent on the flow rate. In addition, it can be seen that there is a small difference (around 1 %) between the best performing solutions (Tank 1B and Tank 1D). The maximum difference in COP for the cases having a diffuser was 4.5 %, when comparing "Tank 1C high" and "Tank 1D high", which occurred due to different amounts of mixing inside the tank. Comparing the best performing diffuser cases (Tank 1D) to a case without a diffuser (Tank 1A high), an increase of up to 32 % can be obtained in the COP of the system.

During discharge, since the temperature range of the tapped water is from 75.3 to 60  $^{\circ}\text{C}$  and the water entering the bottom of the tank is 35  $^{\circ}\text{C}$ , it can be expected that due to mixing, it will not be possible to discharge the entire volume of the tank. That will lead to an amount of energy being left in the tank. This residual energy is presented in Table 6 for each simulated scenario. It can be observed that the solutions having the highest COP are the ones having the lowest residual energy in the tank at the end of the discharge. This is also an indication of the amount of mixing in the tank, since lower mixing with the cold water entering the bottom of the tank leads to more energy being tapped and thus less residual energy in the tank.

Table 6: COP and residual energy calculation for  $h/d=3.64$  tank for high and low flow rate

Case	COP <sub>1</sub>	COP <sub>2</sub>	Residual Energy [kWh]
Tank 1A high	3.50	2.45	1.28
Tank 1B high	3.56	3.20	0.40
Tank 1C high	3.55	3.09	0.53
Tank 1D high	3.49	3.23	0.34
Tank 1A low	3.51	2.95	0.65
Tank 1B low	3.51	3.22	0.35
Tank 1C low	3.52	3.16	0.41
Tank 1D low	3.46	3.23	0.34

Similar results were obtained for tanks having  $h/d=2$  and are presented in Figure 26 and Figure 27, and the corresponding COPs in Table 7. The results for  $h/d=1$  tanks are presented in Figure 28 and Figure 29, and the corresponding COPs in Table 8.

Table 7: COP and residual energy calculation for  $h/d=2$  tank for high and low flow rate

Case	COP <sub>1</sub>	COP <sub>2</sub>	Residual Energy [kWh]
Tank 2A high	3.48	1.92	1.73
Tank 2B high	3.58	3.13	0.46
Tank 2C high	3.56	2.98	0.67
Tank 2D high	3.57	3.17	0.43
Tank 2A low	3.51	2.69	0.96
Tank 2B low	3.55	3.17	0.40
Tank 2C low	3.52	3.07	0.53
Tank 2D low	3.52	3.18	0.42

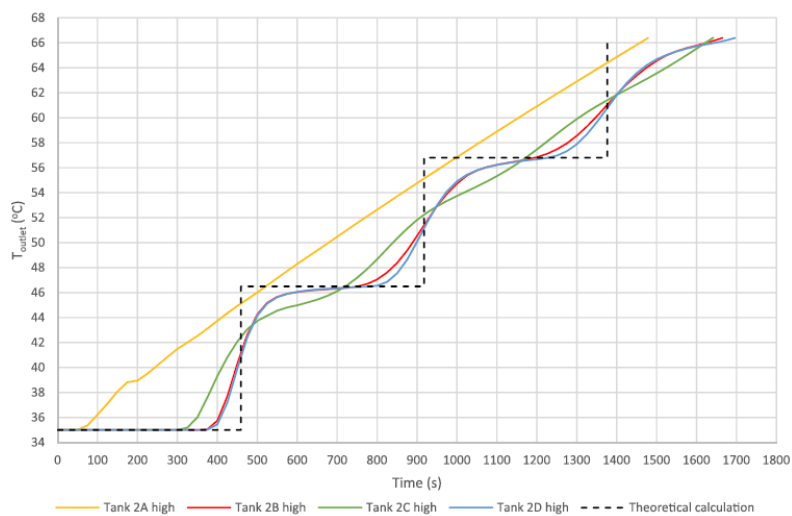


Figure 26: Average temperature at tank outlet during charge – high flow rate ( $h/d = 2$ ).

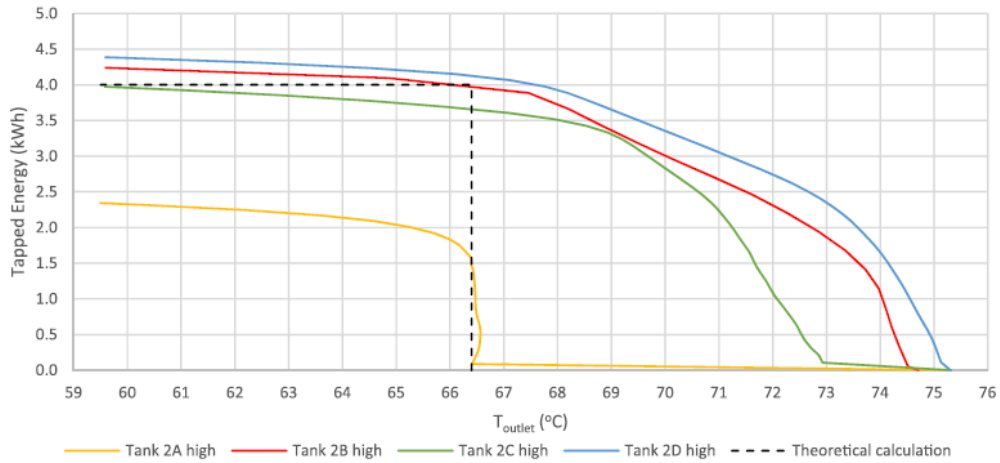


Figure 27: Tapped energy during discharge for a given outlet temperature – high flow rate ( $h/d=2$ ).

Table 8: COP and residual energy calculation for  $h/d=1$  tank for high and low flow rate

Case	COP <sub>1</sub>	COP <sub>2</sub>	Residual Energy [kWh]
Tank 3A high	3.38	0.98	3.35
Tank 3B high	3.51	3.04	0.55
Tank 3C high	3.46	2.82	0.84
Tank 3D high	3.48	3.09	0.52
Tank 3A low	3.39	2.22	1.46
Tank 3B low	3.47	3.07	0.56
Tank 3C low	3.44	2.95	0.68
Tank 3D low	3.46	3.13	0.48

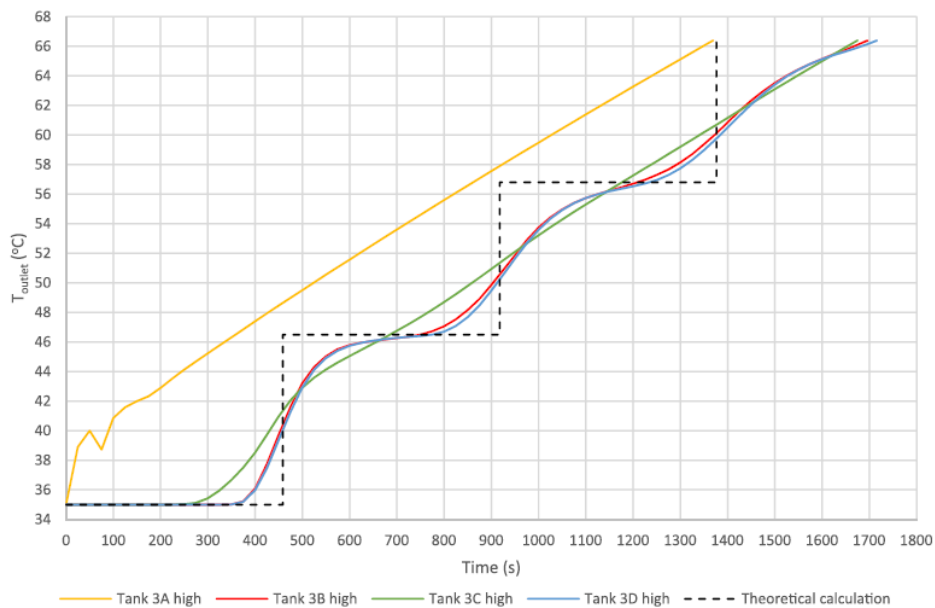


Figure 28: Average temperature at tank outlet during charge – high flow rate ( $h/d = 1$ ).

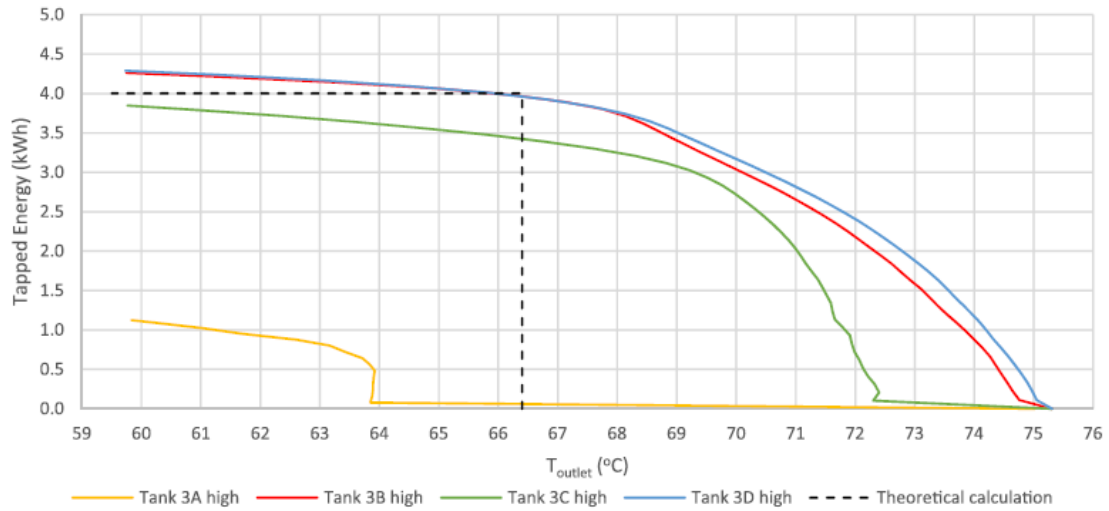


Figure 29: Tapped energy during discharge for a given outlet temperature – high flow rate ( $h/d=1$ ).

An ideal case without any tank material was tested. The absence of material meant that the simulated case had no heat transfer between the water and tank wall and no possibility to store heat in the tank walls. As it can be seen in Figure 30 and Figure 31, the “No material-Tank 1D high” case, came very close to the “ideal case”. The difference between the “ideal case” and the simulation occurs due to mixing inside the tank and thermal conduction downwards in the tank water.

In Table 9, the simulated case having the highest COP is presented, along with the same case without tank material and the “ideal case”. It can be observed that when there is no heat transfer between the water and tank wall, no vertical conduction, and no mixing inside the tank (ideal case), the system COP after a charge-discharge cycle is 3.69. When the effect of mixing and vertical thermal conduction in the water are taken into account (No material-Tank 1D case), even if the case is optimized regarding mixing, the obtained COP is decreased by approximately 9 %. If heat transfer to the tank wall is also taken into account (Tank 1D high case), then the obtained COP is lowered by another 5 % (so approximately 14 % in total). In addition, in Table 9 it can be seen that the “ideal case” is the only one that has a  $COP_2$  larger than  $COP_1$ . The reason for this is that it is the only case where the entire volume of the tank can be discharged since there is no mixing with the cold water and no heat transfer to the tank walls. This fact combined also with the low electricity consumption (since it takes less time to charge the tank compared to the simulated cases) led to a higher  $COP_2$ . It can also be observed that the “ideal case” is able to discharge the whole volume of the tank leaving no residual energy due to the absence of mixing, while this is not the case for the other solutions.

Table 9: COP and residual energy comparison between best performing cases

Case	$COP_1$	$COP_2$	Residual Energy [kWh]
Tank 1D high	3.49	3.22	0.34
No material – Tank 1D high	3.54	3.38	0.2
Ideal Case	3.65	3.69	0

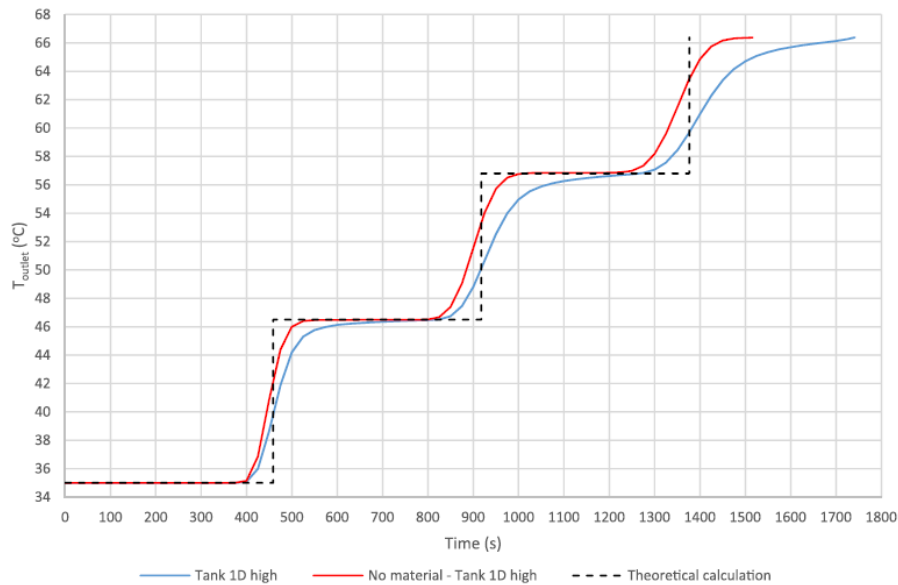


Figure 30: Average temperature at tank outlet during charge for cases with and without tank material – high flow rate ( $h/d=3.64$ ).

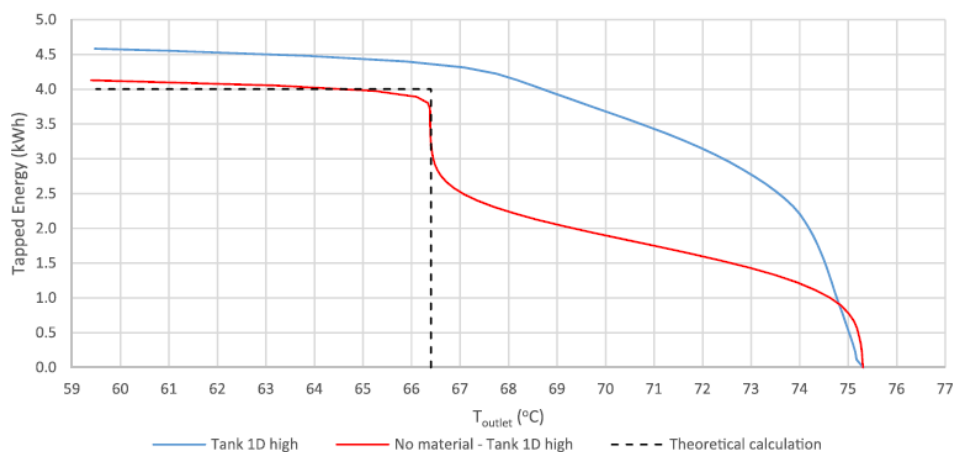


Figure 31: Tapped energy during discharge for a given outlet temperature for cases with and without tank material – high flow rate ( $h/d=3.64$ ).

#### 4.5. Conclusions on small tanks, heating operation

- There is a direct connection between the stratification in the tank and the COP of the system, as a higher degree of thermal stratification leads to a higher COP.
- For the ideal case where there is no mixing and no vertical thermal conduction in the tank and no heat loss from the tank, the system COP after a charge-discharge cycle is 3.69. When the effect of mixing is taken into account, the obtained COP of the system is decreased by approximately 9 %. If heat transfer to the tank wall and vertical thermal conduction are also taken into account, the obtained system COP is lowered by another 5 %.
- The COP of a heating system with high flow rates can be significantly increased by a diffuser plate installed in the tank with a small distance to the inlet/outlet.
- The maximum difference in COP for the cases having a diffuser was 4.5 %, when comparing "Tank 1C high" and "Tank 1D high", which occurred due to different amounts of mixing inside the tank.
- Comparing the best performing diffuser cases (Tank 1D) to a case without a diffuser (Tank 1A high), an increase of up to 32 % can be obtained in the COP of the system.

- The best performing system studied was the system based on an insulated tall and slim tank with a high  $h/d$  ratio of 3.64 and a perforated plate diffuser.
- The best performing diffuser consisted of a 2 mm thick plate with a porosity of 5 %, corresponding to 66 holes of a diameter 0.0075 m spread uniformly over the plate area. The diffuser had also a small non-perforated cyclic region with a diameter of 0.044 m in front of the inlet, in order to block the direct inlet of water jet in the tank.
- The performance of the suggested system was not affected by the tested variations in flow rate.

## 5. Small tanks cold side

Only Case 1 (40 – 9.7 °C) and Case 4 (25 – 2.6 °C) were simulated using CFD. During discharge, the “stop” temperature was 17 °C. The tank volume was approximately 110 l, similar to heating operation. The water flow rate in the system was 0.24 kg/s. The temperature at the tank’s outlet during charge and discharge are presented in Figure 33 and Figure 34 respectively, and the corresponding COPs in Table 10.

Table 10: Performance of Case 1 and Case 4 – cold side

	Case 1	Case 4
COP <sub>1</sub> [-]	4.98	4.01
COP <sub>2</sub> [-]	4.41	6.6
Residual Energy [kWh]	0.386	0.104

The correlation between the tank’s inlet and outlet temperature based on the heat pump operation for cooling for Case 1 and Case 4 is illustrated in Figure 32.

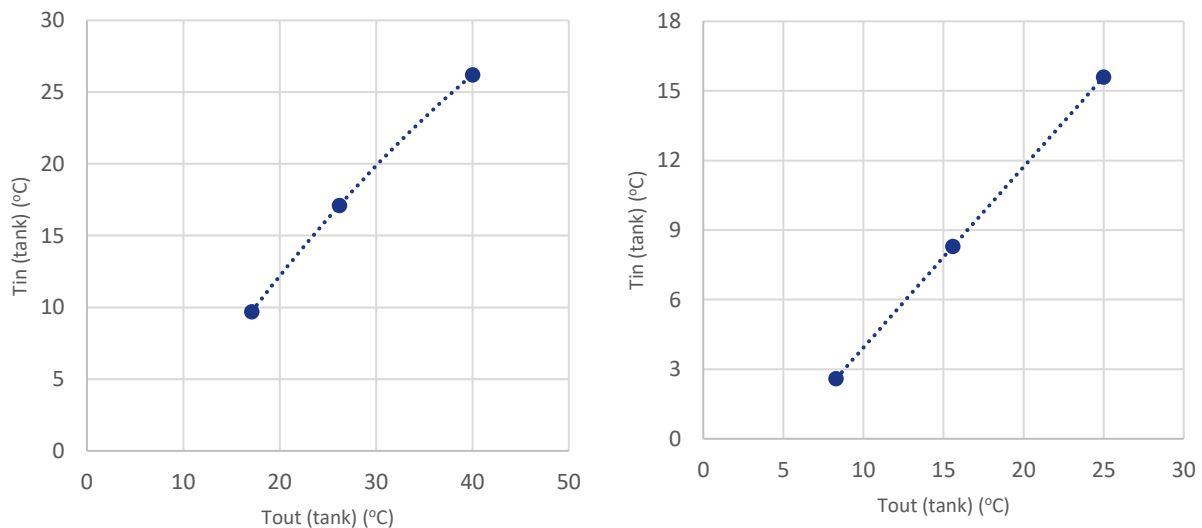


Figure 32: Correlation between tank’s inlet and outlet temperature based on heat pump operation for (a, left figure) Case 1 and (b, right figure) Case 4.

Case 4 has a much higher COP because the discharge temperature (17 °C) is much closer to the initial temperature of the tank (25 °C). Generally, it is difficult to compare in a “fair” way these two scenarios for two main reasons:

- 1) The temperature range is different ( $\Delta T_1 = 30.3$  °C while  $\Delta T_4 = 22.4$  °C)
- 2) The  $\Delta T$  of each pass through the heat pump is different (Case 1 approx. 10.1 °C while Case 4 approx. 7.5 °C).

In order to get a better idea of the amount of mixing inside the tank, the Richardson number for each time-step of the calculation was calculated both for charge and discharge operation.

If the Richardson number is higher than 1, then the buoyant forces are stronger than the mixing forces inside the tank. It can be seen in Figure 35 that Ri number is much higher than 1 indicating low levels of mixing in the tank. The only case where the Ri number gets close to 1 is towards the end of the Case 4 charge. This happens because the temperature is close to 3 °C and density differences become very small.

Generally, it could be said that the tank is satisfactorily stratified, and, thus, even when the temperature approaches 0 °C (and thus density differences are small) there is still a stratified result.

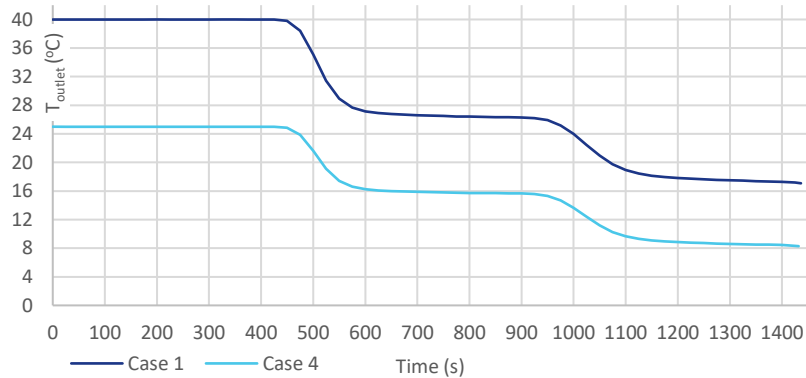


Figure 33: Average temperature at tank outlet during charge – cold side.

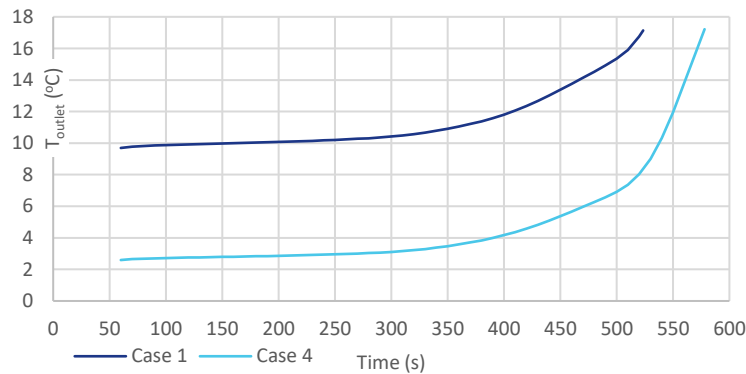


Figure 34: Average temperature at tank outlet during discharge – cold side.

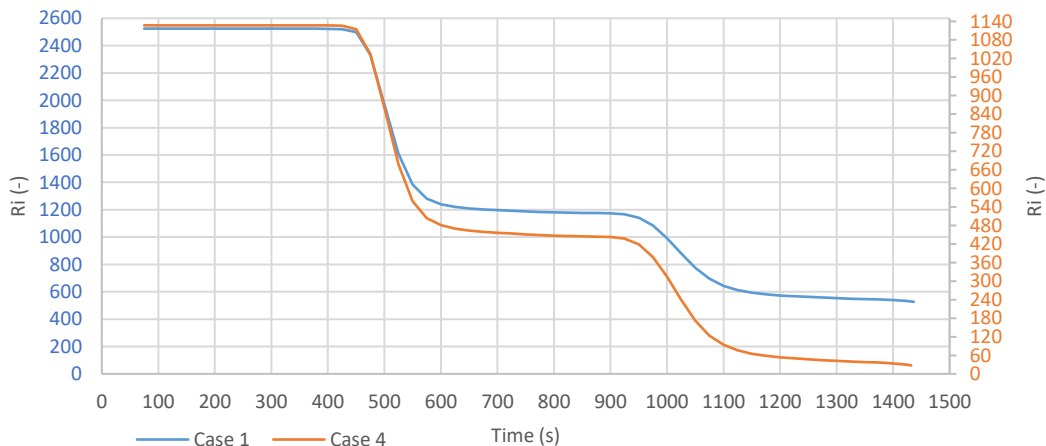


Figure 35: Richardson number during charge – cold side.

Various  $h/d$  ratios were investigated for Case 4 ( $T = 25 - 2.6$  °C), as well as a case with no tank material. The average temperature at tank outlet during charge is presented in Figure 36 and the corresponding COPs in Table 11.

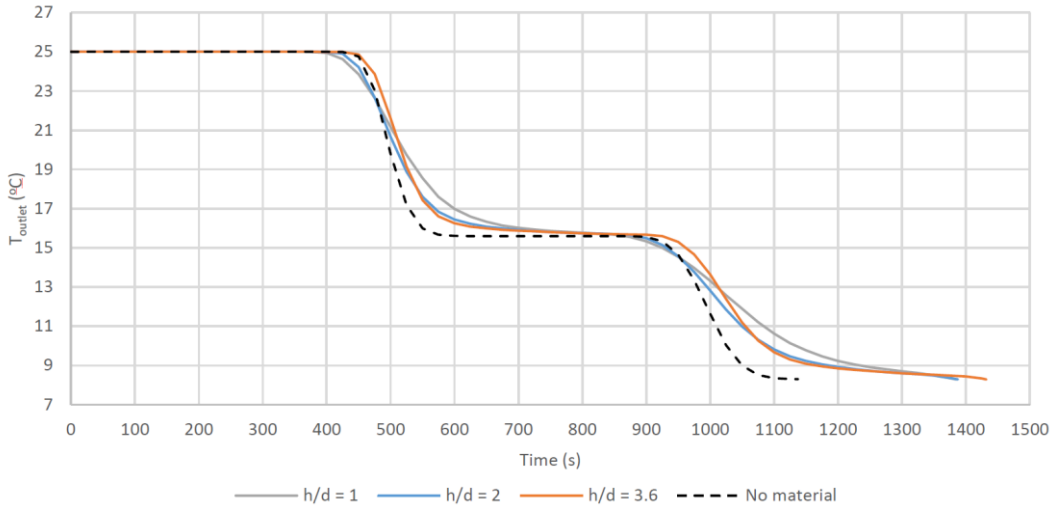


Figure 36: Average temperature at tank outlet during charge – cold side for various  $h/d$  ratios.

Table 11: Performance of Case 4 for various  $h/d$  ratios

	COP <sub>2</sub>	Residual energy [kWh]
$h/d = 1$	2.71	0.15
$h/d = 2$	2.72	0.13
$h/d = 3.6$	2.8	0.1
$h/d = 3.6$ (no material)	2.96	0.05

Case 1 was also investigated for 2 passes of water through the heat pump, instead of three, meaning that the cooling range of this operation would be from 40 – 17 °C (instead of 40 – 9.7 °C). The discharge range was from 17 – 26 °C. This process was investigated for 3 full cycles of charge-discharge and is presented in Figure 37 and Figure 38.

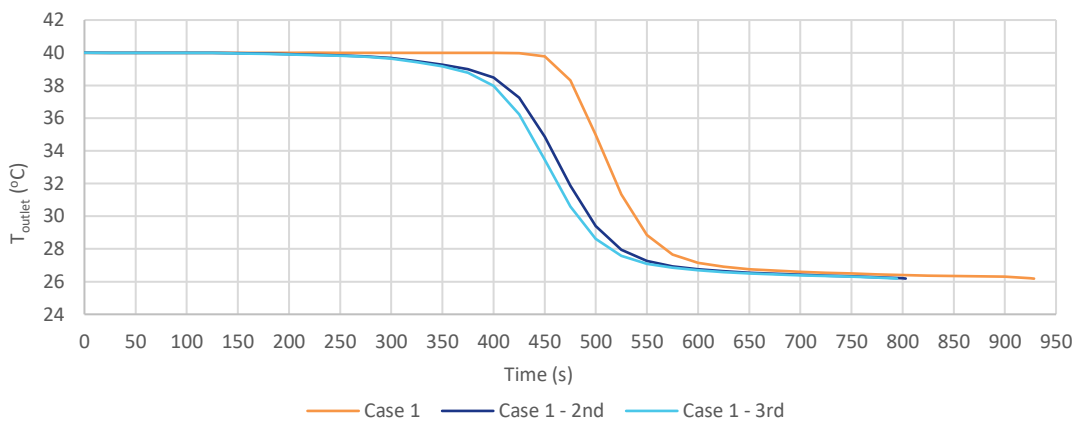


Figure 37: Average temperature at tank outlet during charge – cold side for multiple operation cycles.

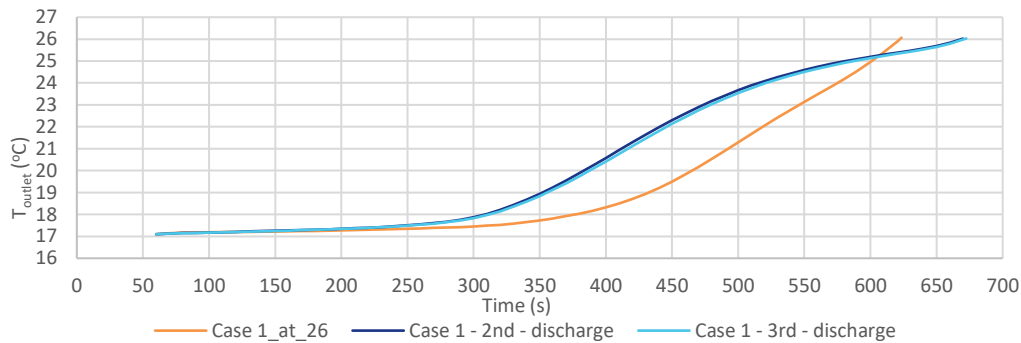


Figure 38: Average temperature at tank outlet during discharge – cold side for multiple operation cycles.

The obtained COP<sub>2</sub> and residual energy of Case 1 (40 – 17 °C) for multiple charge-discharge cycles are presented in Table 12.

Table 12: Performance of Case 1 for multiple charge-discharge cycles

	COP <sub>2</sub>	Residual Energy [kWh]
Case 1 – 2 passes – charge- 1 <sup>st</sup>	4.32	-
Case 1 – discharge – 1 <sup>st</sup>	3.90	0.22
Case 1 – 2 passes – charge – 2 <sup>nd</sup>	4.33	-
Case 1 – discharge – 2 <sup>nd</sup>	4.16	2.35
Case 1 – 2 passes – charge – 3 <sup>rd</sup>	4.32	-
Case 1 – discharge – 3 <sup>rd</sup>	4.25	2.36

## 5.1. Conclusions on small tanks, cooling operation

- Similar to heating, a tall-slim tank gives the best stratification.
- The absence of tank wall material (no heat capacity, no thermal conductivity) gives the highest COP for both cooling and heating operation.
- The differences in obtained COPs for tanks of various h/d ratios are not that profound compared to heating operation.
- Tanks with h/d = 1 and 2 performed almost equally well, unlike heating operation.
- Stratification is not easily established when water temperatures drop below 10 °C due to small differences in water density at these temperatures. However, a tall-slim tank (h/d ≥ 3.64) still manages to produce a stratified profile inside the tank.

## 6. Large tanks hot side

Furthermore, larger systems were investigated, where a 300 kW heat pump was used and tank volumes of 0.5 and 6.5 m<sup>3</sup>. The h/d ratio of these tanks was 3. The flow rate in this system was 7.3 l/sec, and tank charges were from 40 – 80 °C. A similar approach as for the hot side of the small tanks section was followed. Details for the investigated tanks are presented in Table 13.

Table 13: Investigated cases for large tanks hot side

Parameter	Case 1L	Case 4L
Height [m]	1.844	4.221
Diameter [m]	0.615	1.407
Volume [m <sup>3</sup> ]	0.547	6.563
Duration of charge operation [min]	5	60

Cases 1 and 4 were simulated using CFD, having a perforated plate diffuser. Scenarios with no tank material, for investigating the effect of the material on the results, were also performed. The obtained COP<sub>2</sub> and residual energy are presented in Table 14.

Table 14: Material effect on cases 1L and 4L

Cases	COP <sub>2</sub>	Residual Energy [kWh]
Case 1L – perf. plate	4.53	2.94
Case 1L – perf. plate – no material	4.59	2.87
Case 4L – perf. plate	4.75	55.5
Case 4L – perf. plate – no material	4.81	52

Due to the high flow rate, it was decided to attempt to optimize the diffuser plate for Case 4L. The examined parameters for optimizing the diffuser were:

- The position of the diffuser plate (0.02 m, 0.08 m and 0.2 m from the inlet)
- The porosity of the plate (1 %, 5 %, 10 %, 20 %)
- Keeping constant the plate width (0.002 m) and the diameter of the holes of the plate (0.011 m).

In Figure 39 and Figure 40, the average temperature at the tank outlet during charge is presented for perforated plates having 1 % and 5 % porosity for various distances from the inlet. The names of the curves, e.g. P\_1\_D\_02, correspond to a perforated plate of 1 % porosity at a distance of 0.02 m from the inlet/outlet of the tank etc.

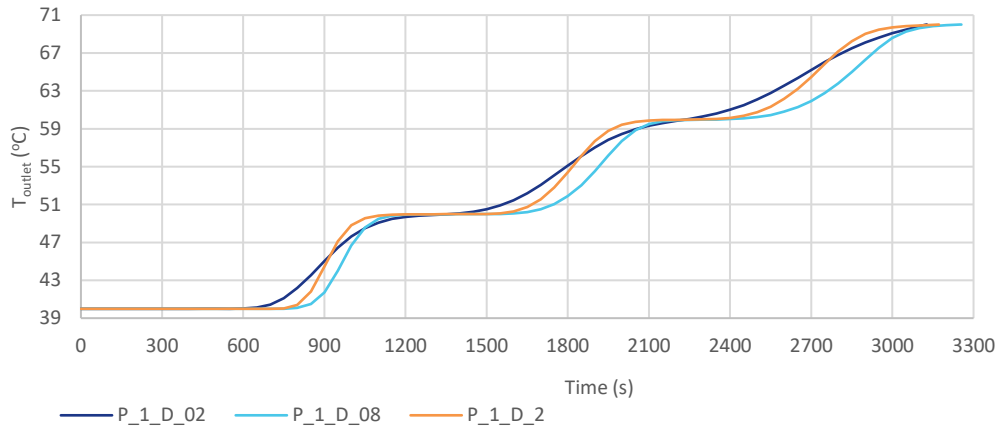


Figure 39: Average temperature at tank outlet during charge - 1% porosity for various distances from the inlet.

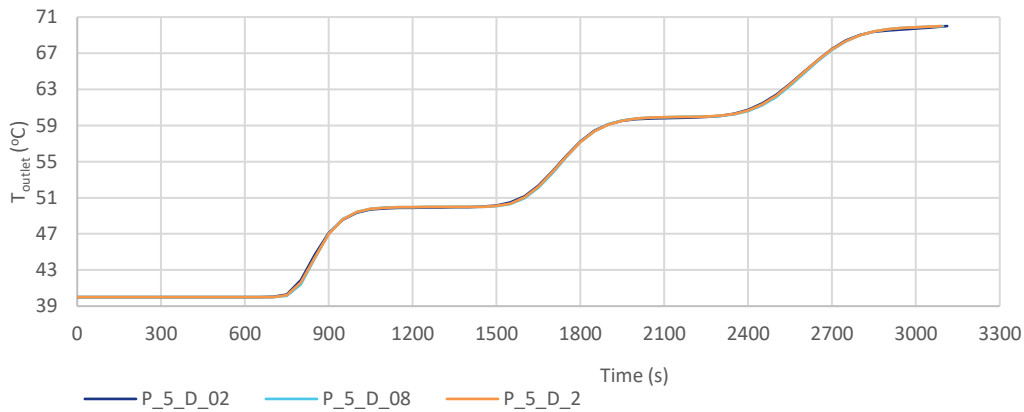


Figure 40: Average temperature at tank outlet during charge - 5% porosity for various distances from the inlet.

The same results were obtained for cases having 5%, 10% and 20% porosity and for that reason they are not presented. In addition, only the case having 1% porosity seems to be affected by the distance of the perforated plate from the inlet, where a distance of 0.08 m seems to give the lowest temperature compared to the other two and thus the lower COP. Selecting this distance all the porosity scenarios were investigated, calculating the corresponding COP. The results are presented in Table 15.

Table 15: Performance of perforated plates at a 0.08 m distance from the inlet/outlet for various porosities

	1% -0.08 m	5% - 0.08 m	10% - 0.08 m	20% - 0.08 m	Ideal Case
COP <sub>2</sub> [-]	4.74	4.67	4.67	4.66	5.67
Total pressure in tank [bar]	1.6	0.06	0.04	0.04	0
Residual Energy [kWh]	31.8	32.5	32.5	44.6	0

Due to the high flow rate, the diffuser plate having 1 % porosity created a much larger pressure inside the tank compared to the other cases. For this reason, in an attempt to decrease the pressure, some scenarios were simulated having two perforated diffuser plates. The plates' characteristics were selected after a sensitivity analysis as the combination that increased the COP without increasing the total pressure in the tank. The first plate had a 10 % porosity at a distance of 0.02 m from the inlet, and the second had a 3 % porosity at a distance of 0.12 m from the inlet. In addition, scenarios with different

discharge temperatures were investigated. The obtained COPs and residual energy are presented in Table 16.

Table 16: Diffuser performance for various discharge levels for Case 4L

		Discharge to 70 °C	Discharge to 65 °C	Discharge to 60 °C	Discharge to 55 °C	Discharge to 50 °C	Ideal Case
2 perforated plates (10 % + 3 % porosity)	COP <sub>2</sub>	4.74	5.03	5.13	5.18	5.22	5.67
	Residual Energy [kWh]	31.3	18.1	11.2	7.3	4.2	0
	Total pressure tank [bar]	0.08					
1 perforated plate (5 % porosity)	COP <sub>2</sub>	4.67	4.97	5.08	-	-	5.67
	Residual Energy [kWh]	32.5	19.6	13.5	-	-	0
	Total pressure tank [bar]	0.06					

The temperature where the discharge stopped was correlated to the residual energy and COP<sub>2</sub>, as it is seen in Figure 41.

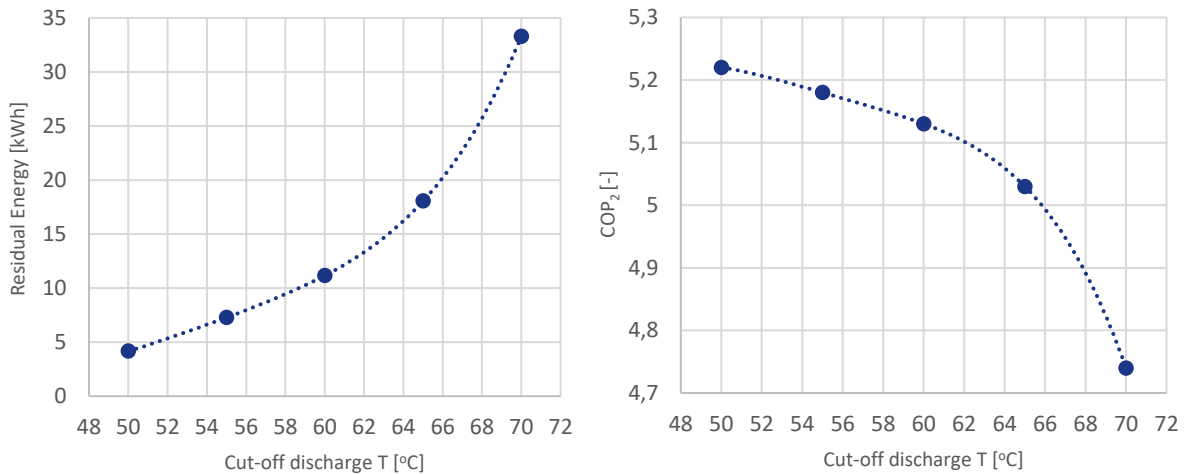


Figure 41: Correlation of the temperature where discharge stopped with (a, left figure) the residual energy and (b, right figure) the COP<sub>2</sub>.

The performance of Case 4L was also investigated for multiple charge-discharge cycles in order to evaluate the system’s COP in real-life operation. The obtained results are summarized in Table 17.

Table 17: COP and residual energy for multiple charge-discharge cycles for Case 4L

	Charge (1 <sup>st</sup> time)	Discharge (1 <sup>st</sup> time)	Charge (2 <sup>nd</sup> time)	Discharge (2 <sup>nd</sup> time)	Charge (3 <sup>rd</sup> time)	Discharge (3 <sup>rd</sup> time)
COP [-]	5.39	4.67	6.07	5.22	6.07	5.22
Residual Energy [kWh]	-	32.54	-	32.53	-	32.53

The reason for the increase in COP after the first charge-discharge cycle is that, due to the residual energy, the initial temperature of the tank is approx. 45 °C (and not 40 °C as in the first cycle). That leads to a smaller charge duration and thus to a lower electricity consumption, giving a higher system COP.

### **6.1. Conclusions on large tanks, heating operation**

- The lowest the diffuser plate porosity is, the better the COP of the system will be due to lower mixing inside the tank.
- A diffuser plate with 1 % porosity has the highest COP but increases the total pressure difference in the tank, reaching 1.6 bar. If a higher porosity of the diffuser plates is used (e.g. 5 % or 10 %), due to higher mixing in the tank, the COP is decreased, but also the total pressure difference is decreased, reaching 0.04 bar.
- A two-perforated-plate scenario (3 % and 10 % porosity) has the same COP as a 1 % porosity plate, while maintaining a low-pressure difference in the tank. However, this solution might increase the cost of the system due to a higher material usage. For this reason, the solution that is recommended for achieving a high performance and maintain a low-pressure difference in the tank at a low cost is a diffuser plate having 5 % porosity.
- Generally, results similar to the small tanks were obtained.

## 7. Testing of concept

### 7.1. Test setup

A test setup has been built. The PI-diagram of this setup is shown in Appendix 2. In Figure 42 and on the front page is shown an illustration of the test setup. Diffusors shown in Appendix 2, Figure A2.3, are mounted in the top and the bottom of the tanks. The system setup has focus on testing the that the concept works as intended and to test the control strategy.



Figure 42: Left: Buffer tank and charge tank. Right: Tanks with sensors mounted.

The cold side of the heat pump is emulated by an electric heater. The control strategy is to keep a constant supply temperature to the evaporator. This is done by having a circuit with a fast flow securing the constant temperature out of the electric heater and a smaller pump supplying the evaporator.

On the warm side of the heat pump, a charge tank with the size of 0.11 m<sup>3</sup> is installed. During the charge period, this tank is heated gradually by circulating water from the bottom to the inlet of the condenser through the condenser and further to the top of the charge tank. The number of circulations before the charge tank is heated to the set point temperature is approximately 10 times.

For the purpose of emulating a large storage tank or an application system, a buffer tank is installed. After the charging period, the water flow is changed in order to discharge the charge tank. The water from the top of the charge tank flows to the top of a buffer tank. At the same time, water from the bottom of the buffer tank flows to the inlet of the condenser continuing through the condenser to the bottom of the charge tank. During this process, a layer of warm water will gradually flow downwards in the buffer tank while the cold water will leave the buffer tank from the bottom. The size of the buffer tank is slightly larger than the charge tank in order to reduce the mixing of the warm top layer and the cold bottom layer and thereby provide a relative uniform temperature when the water is entering the condenser.

## 7.2. Control principle

In the following is given a description of a normal operation of the concept in a commercial operation. Below this are given some extensions which have been necessary for the operation of the test equipment.

The system is intended to be started from a relatively low temperature where the charge tank temperature is lower than the requested outlet temperature. The water is circulated from the bottom of the charge tank through the condenser where it is heated and then to the top of the charge tank. This mode is called the charge tank load mode or just *charge mode* and is given the name D. This operation is continued until a setpoint temperature out of the condenser is reached. During this time, the water in the charge tank has circulated a number of times. The number depends on considerations on the pressure loss and energy for the pumps. In the test, a number of 10 circulations has been used, but it is expected that a smaller number of circulations through the condenser will be sufficient. The temperature difference between the inlet and outlet of the condenser will gradually be decreased. In principle it is possible to decrease the temperature difference between the inlet and outlet even further with the purpose of achieving a more uniform temperature in the tank when the water temperature is close to the setpoint temperature by increasing the flow at this stage.

When the setpoint of the requested temperature in the charge mode is reached, the operation is switched to the *discharge mode*.

In the discharge mode, the flow in the piping is changed. The heat pump is still in full operation, but the outlet from the condenser is now entering the bottom of the charge tank instead of the top of the charge tank. At the same time, the flow from the top of the tank is entering the application system for the use of the heated water. The application system might be a large water storage, or the heated water might flow directly to the application system as supply water. At the same time, return water from the application system will flow to the inlet of the condenser.

In principle, the switch from charge mode to the discharge mode should be as fast as possible. In the tests it has been seen that this shift in temperature did not lead to a major problem. But in principle and probably in some cases the shift might lead to flashing of the refrigerant. To solve this, the temperature could be changed gradually. One way could be by introducing a transition mode where the flow was modified. After advice from a compressor manufacturer, the switch should take about one minute or more. In the start of the transition mode, the flow through the condenser should continue a short while until the temperature of the inlet water to the condenser is reduced to a certain level. When this level is reached, the flow should be reduced considerably. The size of the flow should in principle lead to a gradual reduction of the temperature of the condenser. This is difficult if the water temperature at the inlet to the condenser is varying as a step change. By reducing the flow through the condenser drastically, the temperature difference between the inlet and outlet of the condenser will increase correspondingly. This increase in temperature difference should be so low that the outlet temperature of the condenser will not exceed the requested outlet temperature. This low flow will continue for some time in order to stabilize the conditions in the refrigerant. After some time, the flow can be increased to a higher level leading to a smaller temperature difference. Finally, after some

time, the flow can be increased further to a normal level, and the mode will be the *discharge mode* operation, called mode G.

Due to reasons of optimization of the process, the time for the transition mode should be limited because the efficiency of the process in this mode will be low. This is due to the large temperature difference between the inlet and outlet of the condenser and due to the rapid lowering of the temperature level of the water which destabilizes the refrigerant.

When the setpoint for discharge is reached at the outlet from the charge tank, the flow is changed to charge mode. In this mode, cold water from the bottom of the charge tank flows to the condenser, and from the condenser heated water flows to the top of the charge tank. The heated water entering the top of the charge tank might in the start of the charge mode be colder than the water in the top of the charge tank. There might be a period where water will be mixed in the charge tank. But after maybe one circulation, this mixing will be of a minimum, and the water entering the top of the charge tank will be warmer than the water at lower levels in the tank.

After some circulations, the process is repeated by entering the forced flow mode when the setpoint is reached.

### **7.3. Control in the tests**

For the test, the application system is replaced by a buffer tank. During the charge mode where the charge tank is heated, the buffer tank is prepared to be the water source in the discharge mode. In discharge mode, the top of the buffer tank is supplied with the heated water from the charge tank, and from the bottom of the buffer tank cold water is leaving to the condenser. The preparation of the buffer tank in the charge mode is done by water flow from the top, cooling of this water and letting it enter the bottom of the buffer tank. When an appropriate temperature level is reached in the buffer tank the, cooling is stopped, but the flow from the top to the bottom is continued in order to get the best possible uniform vertical temperature distribution in the buffer tank. In this way, the buffer tank in the end of the charge mode is ready for serving a relative constant inlet temperature during the following transition and discharging mode.

In the test, the reference performance is the situation where the tank temperature has reached the maximum temperature of app. 70 °C.

### **7.4. Operation of Tests**

The tests were carried out under the following framework. The natural refrigerant R600a was used during the operation. The water on the warm side is heated from 30 °C to 70 °C, at the same time as the inlet temperature on the evaporator side is kept constant at 25 °C, and the flow was set to be constant. This means that the temperature of the water out of the evaporator depends on the current condensing temperature. In addition, the subcooler is bypassed during the entire test process. It should be noted that with the refrigerant R600a, the temperature of the saturated liquid is very dependent on the pressure. Here, the R600a differs relatively much from ammonia, which is important to be aware of when comparisons are made with the refrigerant ammonia. In addition, the compressor has been running at a constant speed corresponding to 20 Hz throughout the test.

Figure 43 shows the display of the PLC shortly before the outlet temperature from the condenser reached the set point of the 70 °C, where the shift from the charging of the charge tank to the situation where the content of the charge tank is sent to the buffer tank takes place. The temperatures shown here do not correspond exactly to the temperatures that originates from the data collection. It should also be noted that the temperature stamp in Figure 43 does not precisely match the time stamp indicated on the figures showing graphs from the test.

The mass flows have been maintained throughout the test with 977 kg/h on the warm side and 535 kg/h on the cold side. With the 977 kg/h, a number of circulations of just over 10 is achieved. The evaporator is controlled by an electronic expansion valve with 10 K superheat.

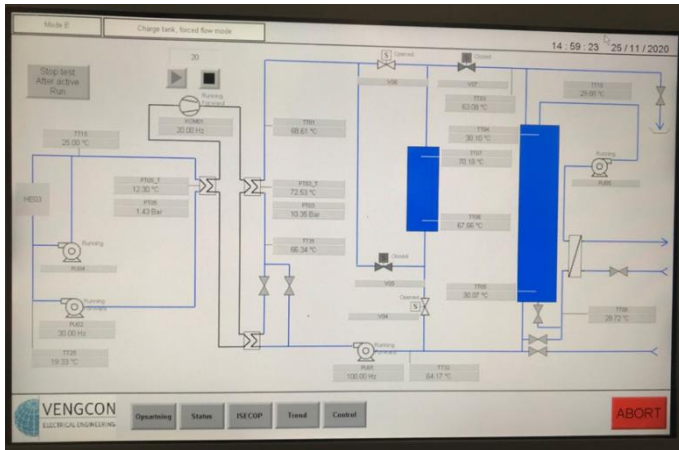


Figure 43: Screen dump of PLC at end of charge mode.

## 7.5. Test Results

Figure 44 shows the results of one of the tests. The temperature of the water out of the condenser (TT14), the condensing temperature (T\_cond\_high\_pressure), the water out of the evaporator (TT03), the evaporation temperature (T\_evap\_low\_pressure) and COP are shown. The measurements are started at 13:43 from a state where the charge tank was charging. The water temperature out of the condenser is approx. 66 °C, and the condensing temperature is approx. 3 K higher. It is also important to note that the evaporation temperature is relatively low due to the undersized evaporator.

Approx. at 13:56, the water out of the condenser has reached the set point of 70 °C, and the discharge process starts. Hereafter, the water flow is changed from being led to the top of the charge tank to now being led into the bottom, whereby the content from the top of the charge tank is now led over to the buffer tank. As soon as this happens, the pump PU05 stops to prevent unnecessary mixing in the buffer tank. This pump is active during the charge process when the cooling circuit for the buffer tank is switched on, and the pump assists also in maintaining as uniform a temperature in the buffer tank as possible.

As can be seen from the graph, the water temperature out of the condenser (TT14) drops relatively quickly due to the fact that the condenser now receives water with a low temperature of approx. 30 °C from the buffer tank. At the same time, the condensing temperature follows the temperature drop of water out of the condenser. The evaporator temperature drops by 5 to 6 K during the shift and then rises again relatively quickly.

Simultaneously with this change, the decrease in the condensing temperature and a reduced power consumption for the compressor, there is a significant increase of the COP.

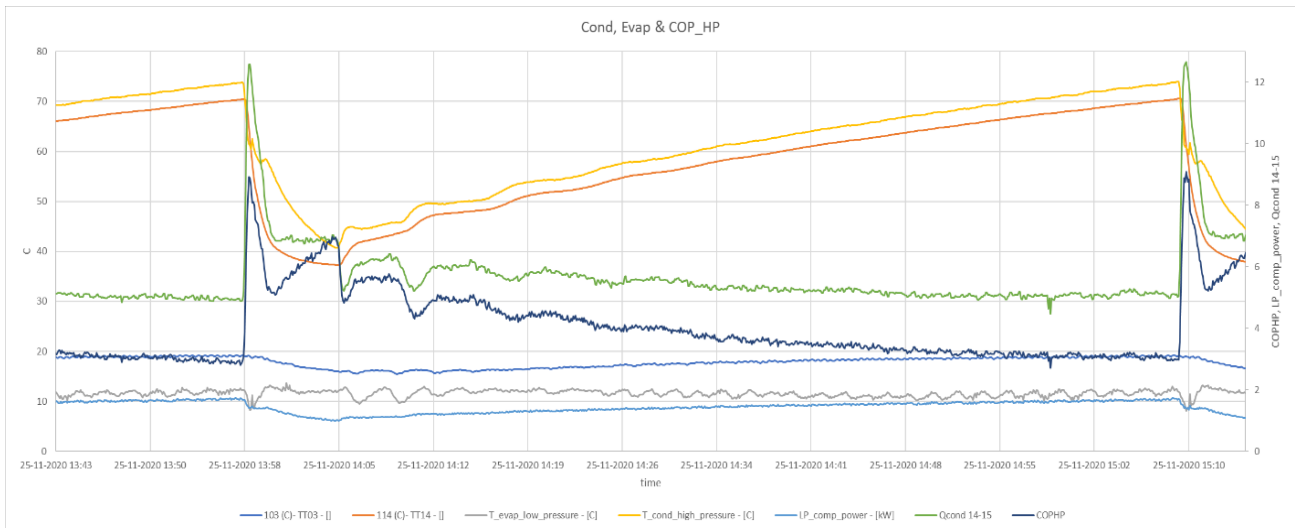


Figure 44: The temperature of the water out of the condenser (TT14), the condensing temperature ( $T_{cond\_high\_pressure}$ ), the water out of the evaporator (TT03), the evaporation temperature ( $T_{evap\_low\_pressure}$ ), the compressor power (LP\_comp\_power), the compressor load (Qcond 14-15) and COP during the test (COPHP).

The capacity of the condenser also makes a huge jump upwards, which is due to the fact that the inlet temperature is falling even faster than the outlet temperature. At 14:05, a volume slightly larger than the charging tank volume has been led to the buffer tank. The slightly larger volume is due to the stop criterion of 60 °C measured with TT03, see Figure 44. Then the mode is changed from discharge to charge, and the water is led to the inlet in the top of the charge tank again, instead of being led to the bottom. At the same time, the flow direction in the charge tank is changed, and the water in the bottom returns to the condenser. At the same time, a temperature jump upwards of the outlet temperature from the condenser is seen. It also appears from the curve that the next charge takes a little less time than in the first cycle. It appears similarly that the staircase shaped change of temperature is washed out over time, which is due to the large flow rate. At 15:09, a whole cycle has been completed.

The efficiency of the heat pump,  $COP_{HP}$ , has a large variation as shown on Figure 44. During the circulation with discharging, the  $COP_{HP}$  increases spike shaped to a value of 9 followed by jump to a value of 5.5, and then the value increases gradually to a value of 7. In the following, the circulation with charging the  $COP_{HP}$  jumps down to a value of about 5 followed by a period with a  $COP_{HP}$  around 5.7. In the end of the second circulation with charging, the  $COP_{HP}$  jumps down again to a value of 4.4. In the third circulation, the  $COP_{HP}$  starts to be 5 followed by a relatively gradual decrease to a  $COP_{HP}$  of 3.0 in the end of the tenth circulation with charging.

An average  $COP_{HP}$  of the heat pump over the whole time interval covering 10 circulations results in a value of 4.1. The temperature in this time interval corresponds to the average temperature in the volume of water that has been transferred to the storage tank of

66.5 °C. This has to be compared with the same heat pump, in an operating point where it delivers a temperature of just 66.5 °C, and it results in a COP<sub>HP</sub> equal to 3.1. It is important to be aware that the heat pump has been running with a subcooling corresponding to somewhere between 5 and 10 K.

The following Figure 45 shows the temperature profile in the charge tank, in the same time interval as in the Figure 44 above. The dimensions indicated below the figure indicate where on the tank the temperature sensors are located, and the upper sensor is indicated as "T\_charge tank 10cm". The fact that the upper temperature sensor shows a temperature lower than in the row below is due to a calibration error. The emptying of the charge tank starts at 13:58. A relatively large number of temperature sensors show a more or less constant temperature, and the higher the position is, the longer they maintain a constant temperature, and the lowest placed temperature sensor is of course the one that first shows a decreasing temperature, caused by this first contact with the cold water which enters the bottom of the tank. At 14:05, the emptying stops, and the inlet to the charge tank shifts back to the top. This also shows that the temperature of the sensor "T\_charge tank 100cm" starts to rise again. The top sensor has a continued falling temperature, which is due to the fact that the water from the condenser has a temperature which is lower than the temperature at the top of the tank. A jump in temperatures can be seen, which is due to the fact that the condenser now gets water delivered from the bottom of the charge tank, which has a higher temperature than the water from the buffer tank. It is clear that a staircase shaped curve is never really established, but that there are zones in the tank with relatively small temperature differences. After the fourth circulation, there is more or less a constant temperature gradient in the tank.

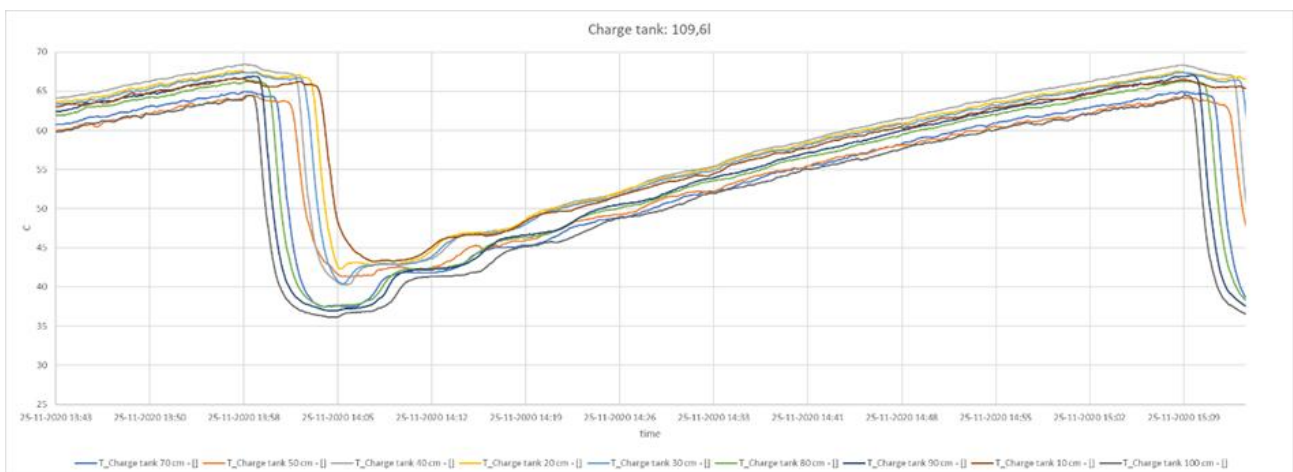


Figure 45: Temperatures in charge tank in same time interval as in Figure 44.

The following Figure 46 illustrates the temperature profile in the buffer (storage) tank. Pump PU05 is not active as long as the buffer tank receives hot water from the charge tank. The temperature in this tank is at the start about 31 °C. The first temperature sensor that detects the hot water is "T\_storage tank - 20cm", which is a bit strange, since the sensor is not located at the highest level.

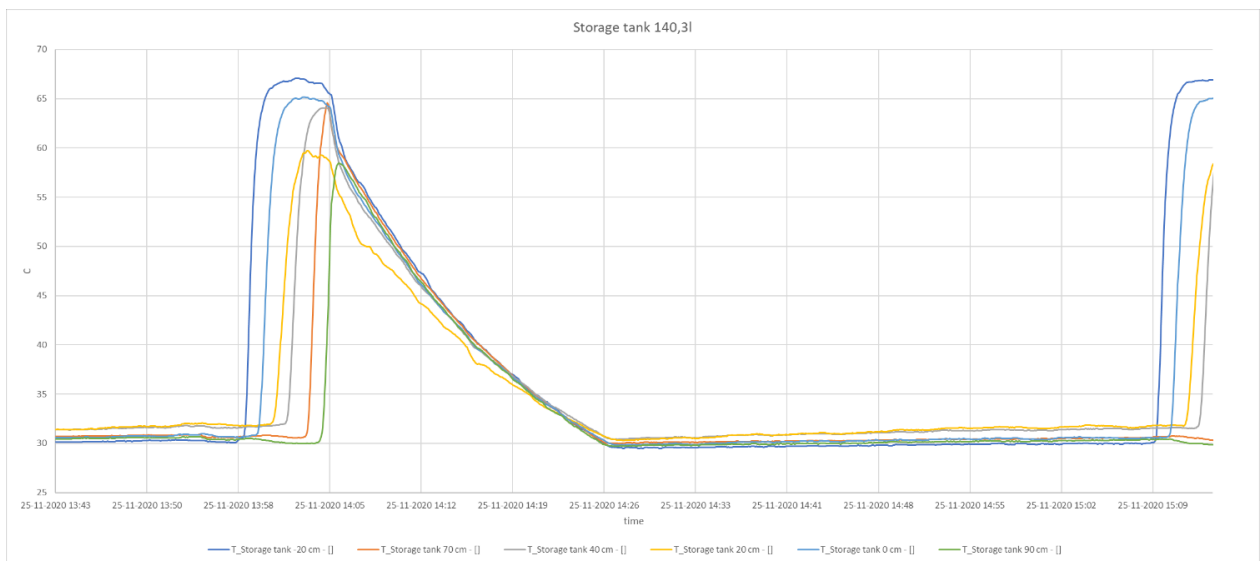


Figure 46: Temperatures in the buffer (storage) tank.

At 14:05, the circulation pump PU05 starts, and the water flows from the bottom of the buffer tank through a heat exchanger where the water is cooled and sent back to the top of the tank. The figure shows the temperature development of the water that flows into the buffer tank. When the emptying of the charge tank stops, then the temperature of the water is approx. 66 °C. At 14:26, the cooling of the tank stops, and the circulation pump is running until the next shift.

## 8. Conclusion

The aim of the project is to illuminate the potential by connecting a tank system on the condenser and evaporator side of heat pumps and thereby achieve a lower average condensation temperature and correspondingly a higher evaporation temperature, and thus a higher COP.

There have been several necessary changes during the project, and the starting point was that the concept should have been demonstrated on a larger ammonia plant. For various reasons, the concept is instead proven on a smaller test facility with the refrigerant R600a.

During the project, CFD simulations of the tank system, static and dynamic simulations, as well as measurements on the concept in a test setup are carried out.

Simulations of the tank system have i.a. aimed to look at the possibilities for establishing a temperature stratification in the tank in order to achieve the largest possible COP during a charge. In this connection, the influence of the height / width ratio of the tanks, inlet arrangement, as well as volume flows and speeds have been investigated.

Results from this have i.a. shown that the velocity as well as the design of the inlet arrangement are important in relation to the tank design. As a starting point, it is important to choose as tall and slim a tank as possible. It has also been shown that without a good design of diffusers, relatively large reductions of the COP can occur in case of larger temperature differences between the inlet and outlet of the condenser during a charge.

DTU MEK has carried out both static and dynamic simulations. In relation to the given assumptions, the simulations have shown the best performance when the refrigerant R600a is used. At the same time, the dynamic model has shown that a COP based on the static model is too optimistic.

A test plant with the refrigerant R600a has been equipped with a tank arrangement for evaluation of the concept. The tank system has been designed by DTU BYG, the tanks are built by MetroTherm, installed by Svedan Industri Køleanlæg, and the system has been modified by Egå Smede & Maskinværksted. The heat exchangers are designed and supplied by Alfa Laval, and the control system has been built by Vengcon. Arla Food and Chr. Møller has provided valuable input for the application of the concept.

The purpose of the test facility has i.a. been to show how the compressor works during the relatively large and periodic pressure reductions on the warm side, as well as to elucidate how well the container design can maintain stratification during operation, and not at least demonstrate the great benefits obtained by connecting a tank system to a heat pump with a relatively large temperature rise.

For testing, the following temperature sets were selected: hot side from 30 °C to 70 °C and on cold side from 25 °C to approx. 15 °C. A charging tank of 110 l was used, and the condenser output has averaged around 6 kW.

It proved difficult to maintain a stepwise stratification in the storage tank after just a few circulations, and during the tests, which were carried out with approx. 10 circulations, it was completely disappeared by the last circulation. But despite of this, the system

managed to raise the  $COP_{HP}$  from 3.1, by direct heating in one step, to 4.1 by use of the tank system. This corresponds to an increase in the  $COP_{HP}$  of 32 %.

The fact that the stepwise stratification is relatively quickly diminished in the tank system is not so important as long as there is a relatively small temperature increase per circulation.

The shift from charging to discharging and back to charging again involves a large variation of the momentaneous  $COP_{HP}$ , but the test results show that a large COP is possible both during the discharge mode and during the start of the charge mode. The test results show a ratio of about 2 between the  $COP_{HP}$  with low condenser temperatures compared to the  $COP_{HP}$  at the high condenser temperatures. These results show that it will be possible to operate the system in the whole temperature range with a good efficiency.

However, it is recommended to be careful when a system is designed with this concept in order to obtain a substantial benefit of the concept. The temperature lift should be of a certain level so there is a significant difference between the efficiency at the different temperature levels in the condenser. There should be a sufficient number of circulations to reduce the loss in efficiency during the shift from one charge period to the next. With a relatively large number of circulations, the period with large fluctuations in the efficiency will be relative short compared to the whole charging period with a stable efficiency. In order to keep a relative sharp boundary between the water with different temperatures, considerations regarding the design should be kept in mind. The geometry of the tank should be slim, the water velocities should be sufficiently low, and the inlet arrangement should be designed carefully to reduce the mixing of water.

In all, the results show that it in many cases with a careful design will be possible to achieve an important improvement of the efficiency of heat pumps.

## 9. References

- [1] F. Bühler, T.-V. Nguyen, and B. Elmegaard, "Energy and exergy analyses of the Danish industry sector," *Appl. Energy*, vol. 184, pp. 1447–1459, 2016.
- [2] K. Wang, F. Cao, S. Wang, and Z. Xing, "Investigation of the performance of a high-temperature heat pump using parallel cycles with serial heating on the water side," *Int. J. Refrig.*, vol. 33, no. 6, pp. 1142–1151, 2010.
- [3] T. Ommen, J. K. Jensen, W. B. Markussen, and B. Elmegaard, "Enhanced Technical and Economic Working Domains of," in *Proceedings of the 24th IIR International Congress of Refrigeration*, 2015.
- [4] E. Rothuizen, C. Madsen, B. Elmegaard, M. Olesen, and W. B. Markussen, "High efficient ammonia heat pump system for industrial process water using the ISEC concept - Part I," *11th IIR Gustav Lorentzen Conf. Nat. Refrig. Nat. Refrig. Environ. Prot. GL 2014*, pp. 816–824, 2014.
- [5] L. Olsen, V. Gaunaa, C. Madsen, and M. F. Olesen, "High efficient heat pump system using storage tanks to increase cop by means of the ISEC concept (part II, thermal storage system).," in *Proceedings of the 24th IIR International Congress of Refrigeration*, 2015.
- [6] M. K. Löffler and N. Griessbaum, "Storage devices for heat exchangers with phase change," *Int. J. Refrig.*, vol. 44, pp. 189–196, 2014.
- [7] E. D. Rothuizen, B. Elmegaard, W. B. Markussen, C. Madsen, M. F. Olesen, and M. Ø. Sølvsten, "High Efficient Heat Pump System Using Storage Tanks To Increase Cop By Means of the Isec Concept ( Part 1: Model validation)," *Proc. 24th IIR Int. Congr. Refrig. Inst.*, 2015.
- [8] L. Olsen, C. Madsen, M. F. Olesen, E. D. Rothuizen, B. Elmegaard, and W. B. Markussen, "Highly Efficient Thermodynamic Cycle with Isolated System Energy Charging (ISEC) - Final Report," 2016.
- [9] F-Chart Software LLC., "EES: Engineering Equation Solver | F-Chart Software: Engineering Software," 2019. [Online]. Available: <http://www.fchart.com/ees/>. [Accessed: 06-Mar-2019].
- [10] R. Kofler, B. Elmegaard, and W. B. Markussen, "Numerical models for the design and analysis of heat pumps with gradual heating using a tank system," 2019.
- [11] R. Kofler, B. Elmegaard, C. Madsen, L. Olsen, and W. B. Markussen, "Screening of heat pump performance improvements obtained through gradual heating using a tank system," in *Proceedings of the 25th IIR International Congress of Refrigeration*, 2019, pp. 2591–2598.
- [12] Johnson Controls Denmark, "Sabroe MatchMaster Program COMPa." 2019.
- [13] IPU, "Pack Calculation Pro." 2015.
- [14] R. Kofler, B. R. Kondakindhi, B. Elmegaard, C. Madsen, L. Olsen, and W. B. Markussen, "Performance analysis of a heat pump system providing district heating and cooling through gradual heating and cooling," *Presentation at 5th International Conference on Smart Energy Systems 2019*, 2019. [Online]. Available: [https://smartenergysystems.eu/wp-content/uploads/2019/09/29-4\\_ReneKoflerSESAAU2019.pdf](https://smartenergysystems.eu/wp-content/uploads/2019/09/29-4_ReneKoflerSESAAU2019.pdf).

- [15] Modelica Association, "Modelica Libraries — Modelica Association," 2019. .
- [16] TLK Thermo GmbH & IFT, "TIL 3.4 – Model library for thermal components and systems." 2017.
- [17] Dassault Systèmes, "Dymola Systems Engineering," 2017.
- [18] H. Martin, "A theoretical approach to predict the performance of chevron-type plate heat exchangers," *Chem. Eng. Process. Process Intensif.*, vol. 35, no. 4, pp. 301–310, 1996.
- [19] Alfa Laval AB, "CAS 5 Version 5.62.0.01." 2016.
- [20] I. Sifnaios, J Fan, L. Olsen, C. Madsen, S. Furbo, "Optimization of the coefficient of performance of a heat pump with an integrated storage tank – A computational fluid dynamics study". *Applied Thermal Engineering 160 (2019) 114014*.
- [21] I. Sifnaios, J Fan. "Effect of tank design on COP. Highly Efficient and Simplified Thermodynamic Cycle with Isolated Heating and Cooling – Cost Optimized (ISECOP)". *Department of Civil Engineering, Technical University of Denmark, Brovej 118, 2800 Kgs. Lyngby, Denmark. Report R-432. March 2020*.

## Appendix 1 - Design Guidelines

Based on the results of this project, some guidelines were written regarding the design of the tank and the tank's diffuser, as well as selection of key system parameters for achieving maximum stratification in the tank. These guidelines can be applied for both heating and cooling applications. The parameters that are taken into consideration are:

- The height/diameter ratio of the tank
- The diffuser design
- The tank wall material
- The flow rate
- The duration of the charging of the tank.

### Height/diameter (h/d) ratio

In order to obtain the best possible stratification, tanks with high h/d ratios have to be used. In this report, the tested h/d ratios were 1, 2 and 3.64. The best performing h/d ratio was the highest tested; namely 3.64. It is believed that a higher h/d ratio (e.g. 4) would give even better results. However, since an increase in the h/d ratio would also increase the price of the tank, a rational selection should be done taking also the cost of the tank into consideration.

In general, a tank with a high h/d ratio has larger heat losses compared to one with a low h/d ratio. In this report, though, all tanks were well insulated ( $U=0.22$  [W/m<sup>2</sup> K]), so heat losses had minor effect on the results.

### Diffuser design

All double-plate diffusers create a "dead" water volume between the bottom plate and the bottom of the tank, which cannot be charged or discharged. For this reason, single-plate diffuser designs are superior compared to double-plate, regardless the design, because they can utilize the entire tank volume.

The location of the diffuser plate should be as close as possible to the tank inlet (e.g. 2 cm). This way, the mixing region in the tank is minimized.

For single-plate diffusers, the diffuser plates should have a diameter as large as possible, reaching the tank walls for minimizing the mixing region.

Perforated single plate diffusers give the best stratification and minimize the mixing inside the tank, compared to other single or double plate diffusers. Generally, the lowest the diffuser plate porosity, the better the COP of the system due to lower mixing inside the tank.

A diffuser plate with 1 % porosity has the highest COP but increases the total pressure difference in the tank. If higher porosity diffuser plates are used (e.g. 5 % or 10 %) due to higher mixing in the tank, the COP is decreased, but also the total pressure difference is decreased.

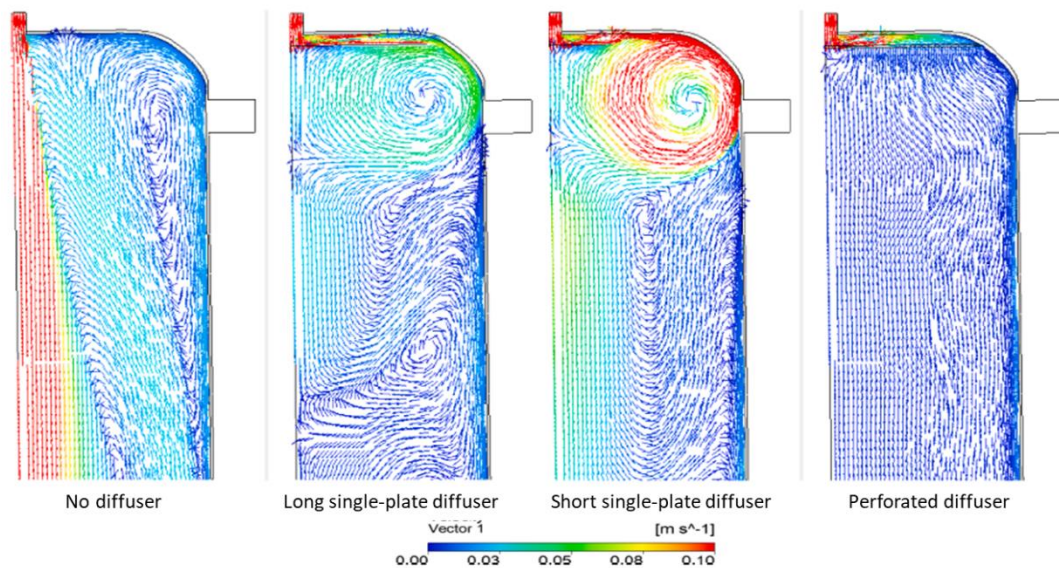


Figure A.1: Velocity vectors at the top part of the tanks during charge for various diffuser designs.

A two-perforated-plate scenario (10 % and 3 % porosity) has the same COP as a 1 % porosity plate, while maintaining a low-pressure difference in the tank. However, this solution might increase the cost of the system due to higher material usage.

For this reason, the solution that is recommended for achieving a high performance and maintain a low pressure difference in the tank at a low cost, is a single diffuser plate having 5 % porosity, corresponding to 66 holes of a diameter 0.0075 m spread uniformly over the plate area. It is also suggested for the diffuser to have a small non-perforated cyclic region with a diameter of 0.044 m in front of the inlet (if the inlet is a  $\frac{3}{4}$ " pipe, otherwise, a larger non-perforated region might be necessary), in order to block the direct inlet of water jet in the tank.

#### Tank wall material

In all the investigated cases, for both heating and cooling operation, absence of tank material was beneficial for stratification. In the simulations, a hypothetical material was used, having zero specific heat capacity and thermal conductivity – meaning that there was no heat transfer between the water and the tank wall, no possibility to store heat in the tank walls, no heat loss and no downward thermal conduction in the tank walls. In a real life scenario, any material with lower specific heat capacity and thermal conductivity than steel or stainless steel, which are mostly used in tanks, would create a better stratification in the tank.

However, a number of other parameters have to be taken into consideration like:

- How much would the material actually increase the performance?
- How large pressure will it have to withstand?
- How stable is it for multiple charge-discharge cycles?
- What is the cost and lifetime of the tank?

**Flow rate**

For a 110 l tank, it was proven that a flow rate in the range of 0.12 – 0.24 kg/s gave the same results, provided that an optimized diffuser is used (e.g. high diameter single-plate or perforated). This proves that, although smaller water velocities create better stratification, with the use of an appropriate diffuser, higher flow rates can be used producing an equally good stratified tank.

**Charge duration**

A charge duration of 20 – 30 minutes is suggested. Longer durations (corresponding probably to lower flow rates) are likely to affect stratification positively, but at the same time heat losses from the tank to the ambient start becoming significant as well as the size of the tanks will become larger.

## Appendix 2. Test setup

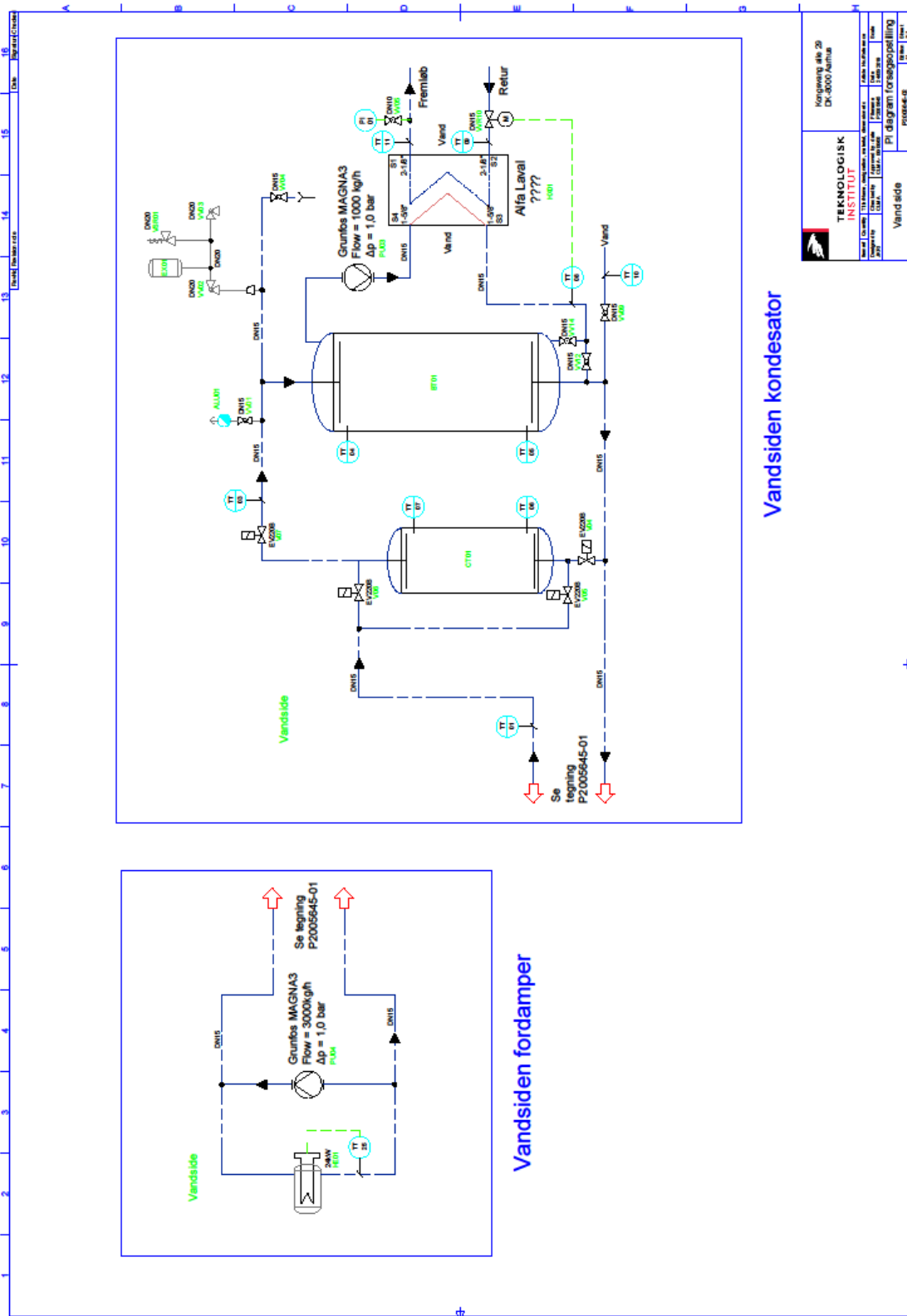


Figure A2.1: PI-diagram for water side of evaporator and condenser.



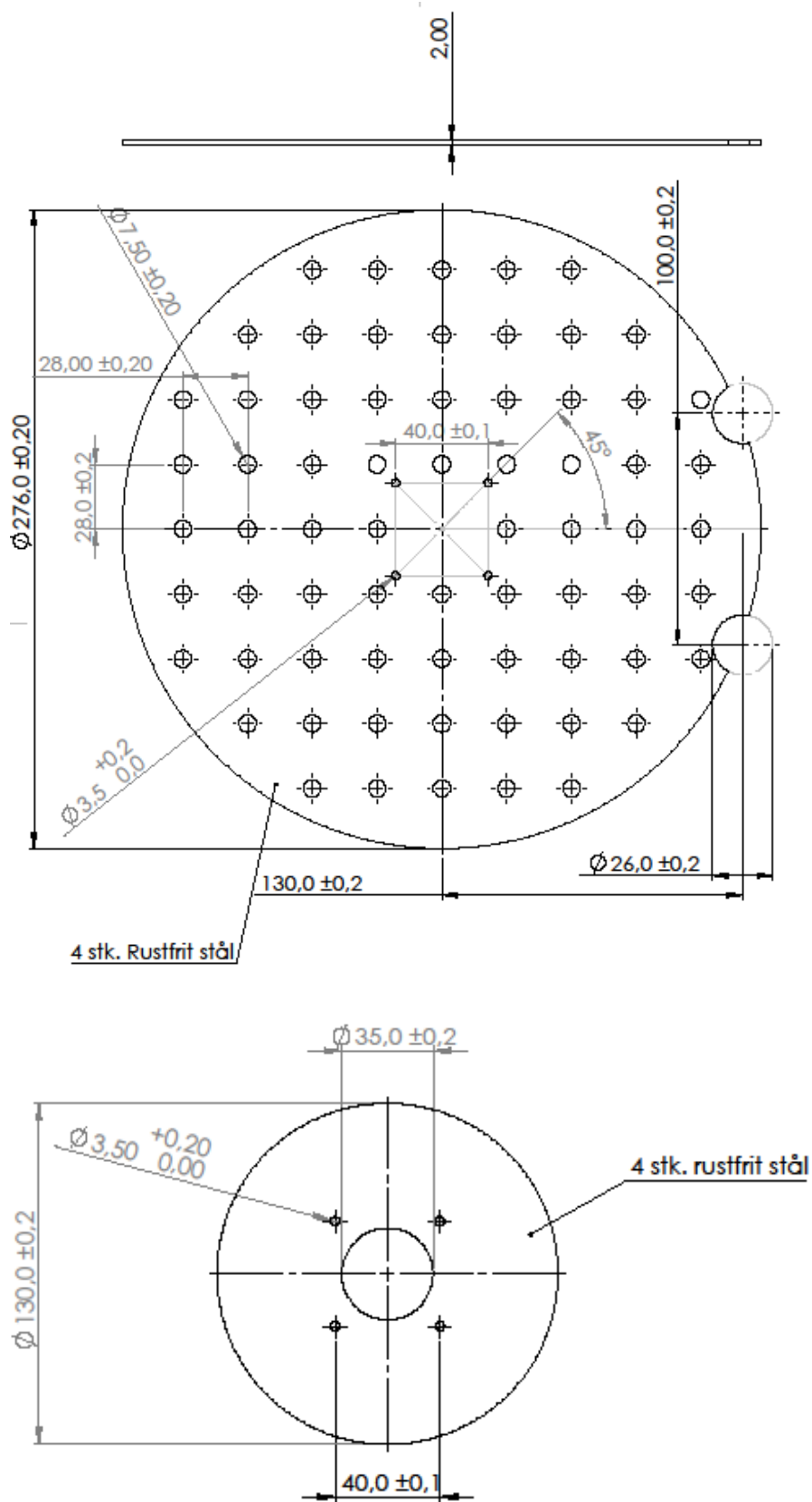


Figure A2.3: Drawing of diffuser plate.

### Appendix 3. Thermographic observations of temperature profiles

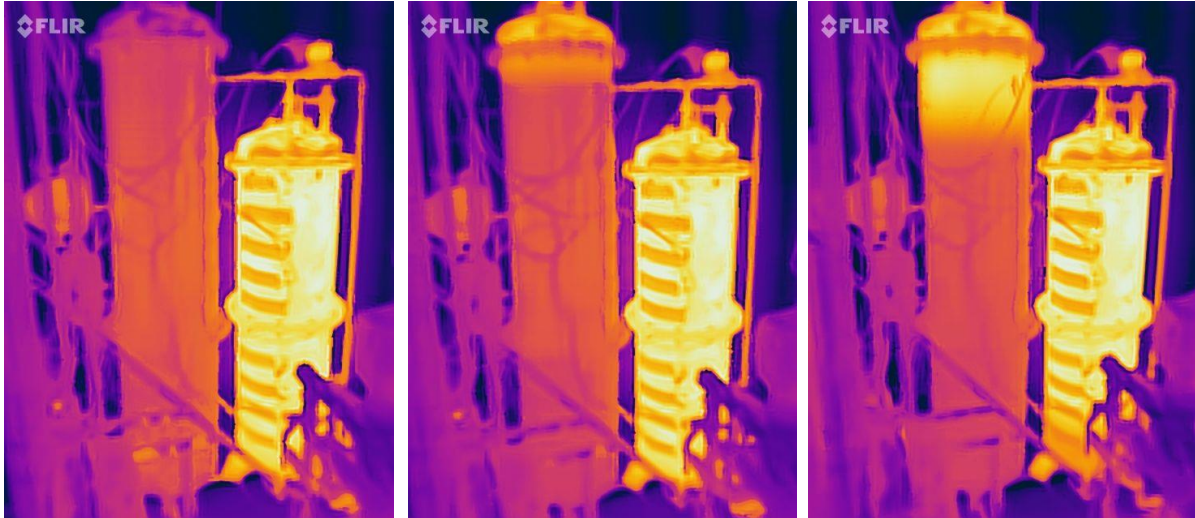


Figure A3.1: Development of temperature profiles in buffer and charge tank. The buffer tank (on the left side, coloured orange) is cold while the charge tank (on the right side, yellow) is warm. The buffer tank is gradually heated from the top while the charge tank is being cooled from the bottom. The operation of the system is in charge mode.

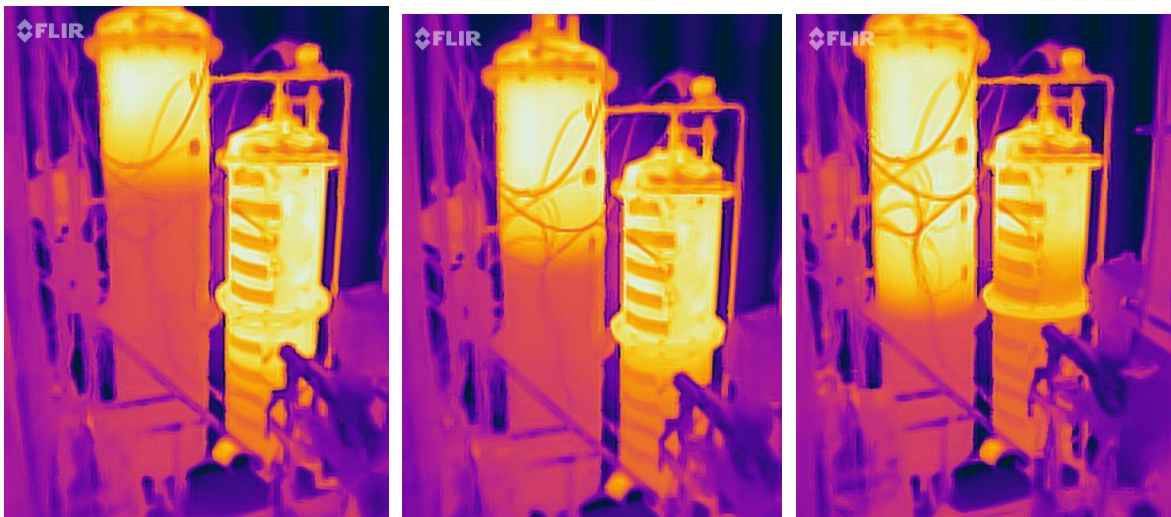
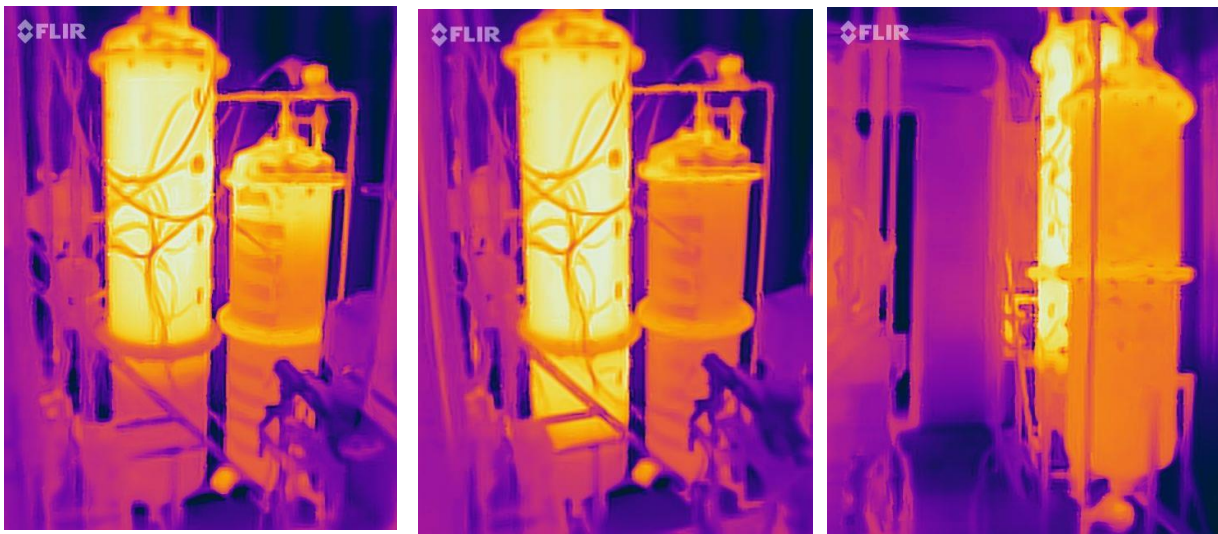


Figure A3.2: Development of temperature profiles in buffer and charge tank. The charging process is being continued. For both tanks, the upper part is warm, and the lower part is cold.



*Figure A3.3: Development of temperature profiles in buffer and charge tank. The charging process is being continued. For both tanks, the upper part is warm, and the lower part is cold.*